Recent advancements in design, development and demands of photothermal superhydrophobic materials

Sijie Cheng [a], Sanjay S. Latthe [a,b], Kazuya Nakata [c], Ruimin Xing [a,**], Shanhu Liu [a,*], Akira Fujishima [d,e]

[a] College of Chemistry and Molecular Sciences, Henan University, Kaifeng, 475004, China
[b] Self-cleaning Research Laboratory, Department of Physics, Vivekanand College (Empowered Autonomous), Kolhapur, 416003, (Affiliated to Shivaji University, Kolhapur), Maharashtra, India
[c] Division of Sciences for Biological System, Institute of Agriculture, Tokyo University of Agriculture and Technology, 2-24-16 Naka-cho, Koganei, Tokyo, 184-0012, Japan
[d] Tokyo University of Science, 2641 Yamazaki, Noda, Chiba, 278-8510, Japan
[e] Institute of Photochemistry and Photomaterials, University of Shanghai for Science and Technology, 516 Jungong Road, Shanghai, 200093, China

ARTICLE INFO

ABSTRACT

Photothermal materials are received considerable attention due to their broad solar absorption and effective light-to-heat conversion feature. Superhydrophobic surfaces are incorporated in diverse applications due to their excellent water repellent performance. With the development of advanced nanotechnology and sophisticated practical demands, the photothermal superhydrophobic materials (PSM) found appealing for exploring prospective and fascinating applications. In this review, we first introduce the recent development and progress in photothermal superhydrophobic materials, with a focus on the mechanism of light-to-heat conversion. The current status is thoroughly discussed, with a detailed catalogue such as metal-based, semiconductor-based, carbon-based, and polymer-based photothermal superhydrophobic materials. The applications of PSM are overviewed on various industrial sectors, including seawater desalination, passive anti-icing/active deicing, crude oil cleaning, photothermal disinfection and photothermal actuation. In the end, future opportunities and challenges in this fascinating research field are tentatively proposed.

1. Introduction

Solar energy is a clean, sustainable and abundant energy source that is expected to replace the inadequacy of traditional energy sources [1,2], and can be utilized directly and/or transformed into other form of energy, such as photothermal conversion [3,4]. Solar radiation is an electromagnetic spectra that consist of abundant photons. When solar photons collide with electrons, it absorbs energy from photons. The absorbed photon energy is released in the other form of energy. On the demand of practical applications, the expected ideal photothermal material should have high solar light absorption across the entire solar spectrum and high light-to-heat conversion efficiency, ubiquitous and sustainable material resources, simple fabrication method and low cost. From the last decade, researchers have paid attention to explore the application of photothermal materials to meet different requirements in

seawater desalination [5], photothermal de-icing [6], photothermal therapy [7] and sewage treatment [8,9].

On the surface of natural lotus leaf, the water droplets freely rolls and clean the surface itself by collecting dust, which is famously referred as "lotus effect". Studies have shown that the "lotus effect" is mainly caused by the micro- and nano-structures and the wax layer with low surface free energy [10–12]. The term "wettability" states the ability of a liquid to moisten a solid surface and the degree to which a liquid adheres to a solid surface. The term 'contact angle' (θ) is introduced when determining the wettability of solid surface, and the wettability is classified into four types depending on the values of contact angles, including superhydrophilic ($\theta < 10°$), hydrophilic ($10° < \theta < 90°$), hydrophobic ($90° < \theta < 150°$) and superhydrophobic ($\theta > 150°$) [13,14]. The wetting phenomenon is well described by Young's model, Wenzel's model and Cassie-Baxter's model on the basis of surface structure of

---

* Corresponding author.
** Corresponding author.
    E-mail addresses: rmxing@henu.edu.cn (R. Xing), liushanhu@vip.henu.edu.cn (S. Liu).

solid surface [15] (Fig. 1). The relevant formulas and theories have been introduced in previous reviews published by us and other research group [16–18]. Young's model [19], which describes the wetting state of a liquid on a perfectly flat and smooth solid surface, takes into account the mathematical relationships between solid-air (γ_{sa}), solid-liquid (γ_{sl}), and liquid-air (γ_{la}),

$$\gamma_{sa} = \gamma_{sl} + \gamma_{la} \cos \theta_Y \tag{1}$$

where, θ_Y is apparent contact angle (Young's angle) between solid-liquid and liquid-air interface. However, most solid surfaces have rough and uneven chemical structures, making Young's model inapplicable. Wenzel [20] modified Young's equation by introducing surface roughness factor (r); written in the form of,

$$\cos \theta_W = r \cos \theta_Y \tag{2}$$

where, θ_W and r are the apparent Wenzel contact angle (Wenzel's angle) and roughness factor, respectively. The roughness factor (r) is the ratio of the actual solid-liquid contact area to the apparent solid-liquid contact area. The value of roughness factor represent wetting type of solid surface. Wenzel model has restricted by thermodynamics balanced state and unique chemical component. Cassie and Baxter [21] have initiated a new mathematical formulation that will be suitable. The Cassie-Baxter equation written in the form of,

$$\cos \theta_{CB} = f_1 \cos \theta_1 + f_2 \cos \theta_2 \tag{3}$$

where, θ_{CB} represents the apparent contact angle of the droplet in the Cassey-Baxter state. θ_1 and θ_2 are the contact angle of liquid droplets on the surface1 and surface2, respectively. f_1 and f_2 are the surface roughness factor corresponds to surface1 and surface2, respective. Therefore, the Cassie-Baxter equation will be suitable for explaining wetting property of rough surface along with existence of air into their small protrusions.

Since the establishment of the basic theory of superhydrophobic surfaces, the research related to superhydrophobic surfaces has been continuously developed (Fig. 2a). The number of research articles on the development of superhydrophobic surfaces were also showed an increasing trend year by year (Fig. 2b). Multi-functional super-hydrophobic materials, such as repairable superhydrophobic materials, stretchable superhydrophobic materials, magnetic superhydrophobic materials, conductive superhydrophobic materials, flame retardant superhydrophobic materials and PSM have been designed [22].

PSM combines photothermal conversion properties with super-hydrophobicity, which not only solve the problem of surface contamination, but also enhance the absorption of solar radiation by repeatedly reflecting and absorbing light. Since 2018, the number of researches based on PSM has increased rapidly (Fig. 2c), and it has been widely used in rapid passive anti-icing and active deicing [23–25], crude oil cleaning [26–29], seawater desalination [30], photothermal actuation [31] and sensing [32], providing a new way of green and environmental

protection instead of the traditional high energy consumption methods. In this review, the recent progress of PSM based on photothermal responsive materials is reviewed, and the preparation and sustainable applications, including seawater desalination, passive anti-icing and active deicing, crude oil cleaning and disinfection are discussed. At last, the current challenges and future prospect of PSM's are briefly summarized.

2. Photothermal superhydrophobic materials: recent development and progress

The construction of a surface with a large water contact angle (WCA) should meet the following conditions: the construction of a micro-structure similar to the surface of the lotus leaf (physical construction), or/and the modification of the structure with a low surface energy chemical, such as fluoroalkyl silane (chemical construction). Random roughness can be induced via physical or chemical means, followed by chemical modification to achieve low surface energy. Among them, chemical modification is a common method to obtain superhydrophobic surface. However, sometimes fluorinated reagents/oleoamines are used for modification, which is harmful to the environment. The methods developed to create superhydrophobic surfaces mainly include lithography, etching, spraying, sol-gel method and layer-by-layer deposition method [33–38].

In lithography, a light source irradiating on a surface coated with a photoresist on a photomask so that fine micro-/nano-structure can be transferred from the master to the substrate. Lithography is highly reproducible and can construct surface structures with accurate shapes and sizes. Etching methods mainly include plasma etching, chemical etching and laser etching. Laser etching has the advantages of non-contact and fast, neither forming pollutants nor requiring complex conditions, and can effectively avoid scratches and damage in the process of processing. Spraying method is to spray solution from the spray gun under a certain pressure to form a mist adhesion on the surface of the substrate. It possesses advantages of simple operation, low cost, suitable for a variety of substrates, and can achieve large-scale production, uniform and smooth spraying effect and good visual effect. Layer-by-layer (LbL) deposition is to add multilayer films on the substrate, which are usually combined with colloidal particles and polymers with alternating charge, and the electrostatic interaction is used to strengthen the overall bonding to obtain strong mechanical stability. LbL deposition is a simple and inexpensive method for the preparation of various coatings, which is suitable for the deposition of thin films on large areas of uneven surfaces. Among electrochemical methods, electrochemical deposition has advantages of high processing efficiency, good surface quality, strong controllability and low cost. Electro-chemical methods are commonly used to prepare superhydrophobic coatings on metals, metal oxides and conductive polymers because of their easy parameter tuning. Physical vapor deposition (PVD) is the sputtering/evaporation of different components under vacuum
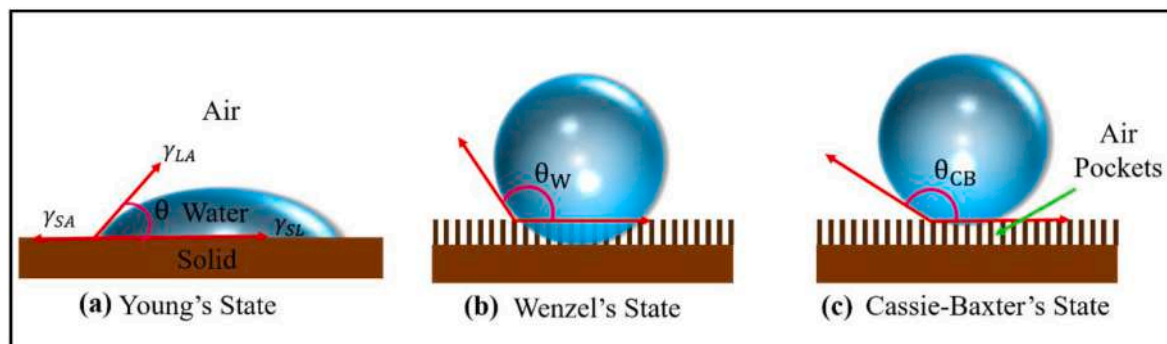

Fig. 1. (a) Young's model. (b) Wenzel model and (c) Cassie-Baxter model.
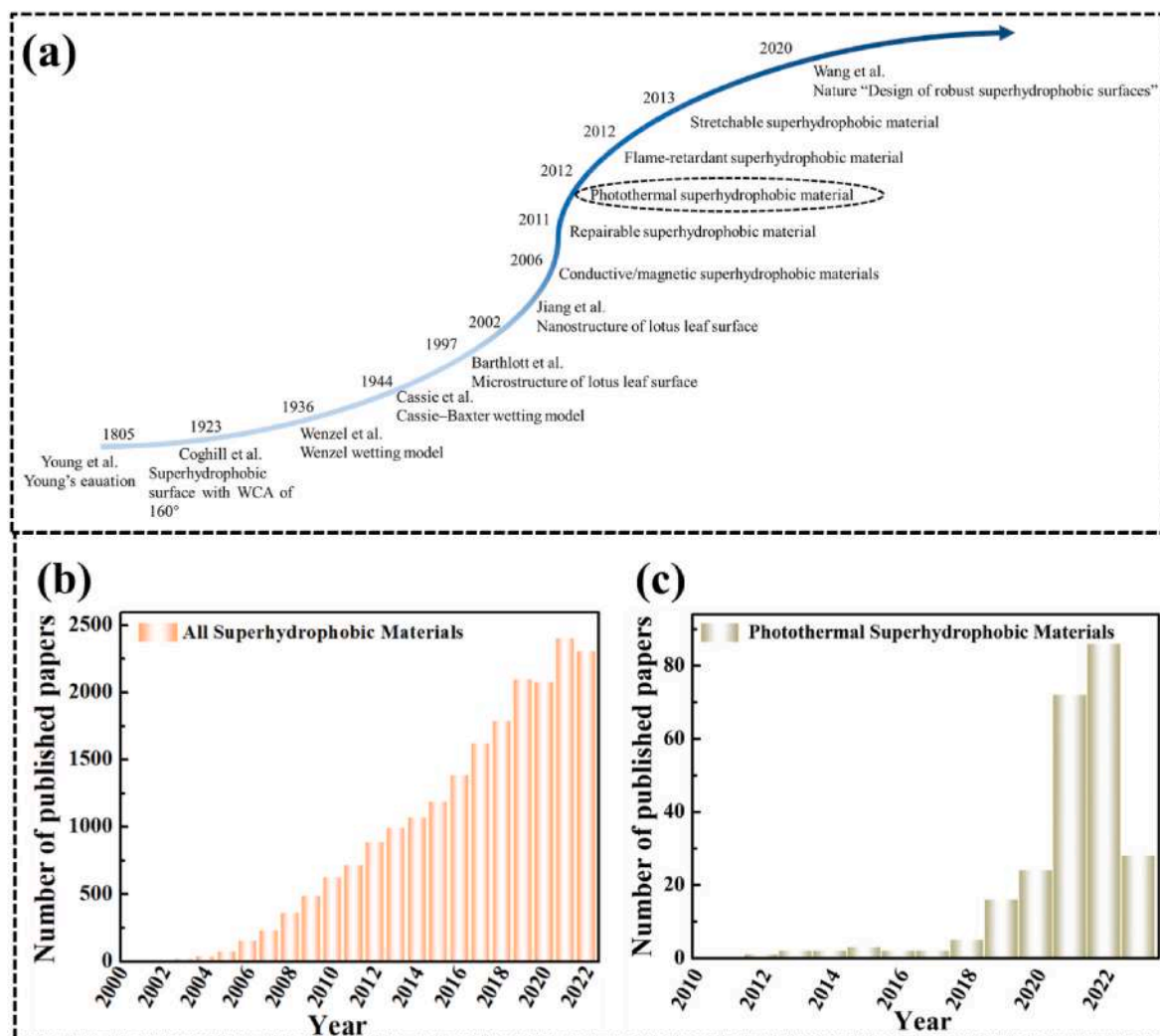
Fig. 2. (a) Development of multifunctional superhydrophobic materials. (b) Number of superhydrophobic materials listed in Web of Science from 2000 to 2022. (c) Number of PSM listed in Web of Science from 2010 to 2022.

conditions to produce gaseous atoms, molecules or partial ionization into ions, and in an inert atmosphere to form a vapor deposition on the surface of the substrate has a special function of the film and heat treatment curing into nanocomposites. PVD has the advantages of simple preparation process, less consumables, uniform and dense film formation, and can use a variety of inorganic materials and some organic materials. The process of deposition of thin films on substrates exposed to gaseous is called chemical vapor deposition (CVD). In the sol-gel method, the precursor (metal compound) is hydrolyzed to form a sol, and then the sol is coated on the surface of the substrate to form a gel, which is further dried to form a three-dimensional porous coating. The sol-gel method has the advantages of easy processing, environmentally friendly, cost-effective, mild operating conditions, and no need for high-energy etching or high-temperature roasting. However, it is worth noting that the shortcoming of the proposed method, which leads to particle aggregation due to high surface energy, greatly limits its application in the desired field.

At present, the preparation of PSM is mainly through two ways: one is to introduce photothermal components into the superhydrophobic material, and the other is to modify the photothermal material by superhydrophobic treatment. Among them, superhydrophobic modification of photothermal materials is a commonly used method in the reported research. According to the different mechanisms of photothermal conversion (plasma heating, electron hole generation, molecular thermal relaxation and thermal vibration) [39–43] (Fig. 3), photothermal materials are often divided into carbon materials, metal nanomaterials, semiconductor materials and polymer materials [44]. Materials used for photothermal conversion have advantages such as broad band absorption in the wavelength range of 300–2500 nm, suitable thermal conductivity, low thermal emission and high stability [45]. Table 1 compares the advantages and disadvantages of PSM for different types of photothermal materials.

2.1. Metals-based photothermal superhydrophobic materials

Metal nanomaterials have been used as effective photothermal conversion materials due to their high strength, high toughness, and excellent thermal stability [46–48]. The photothermal conversion mechanism of metal nanomaterials is the local surface plasmon resonance (LSPR) effect. When the frequency of incident electromagnetic radiation is analogous to that of free electrons in metal, electrons will be collectively excited and produce resonance, which converts kinetic energy into thermal energy and hence local heat increases [49]. The light absorption capacity of metal nanomaterials is affected by material type, morphology, particle size and composition [50]. The rough structure formed by metal nanoparticles on the surface of the material can effectively reduce the surface energy, which is favorable for the formation of PSM.
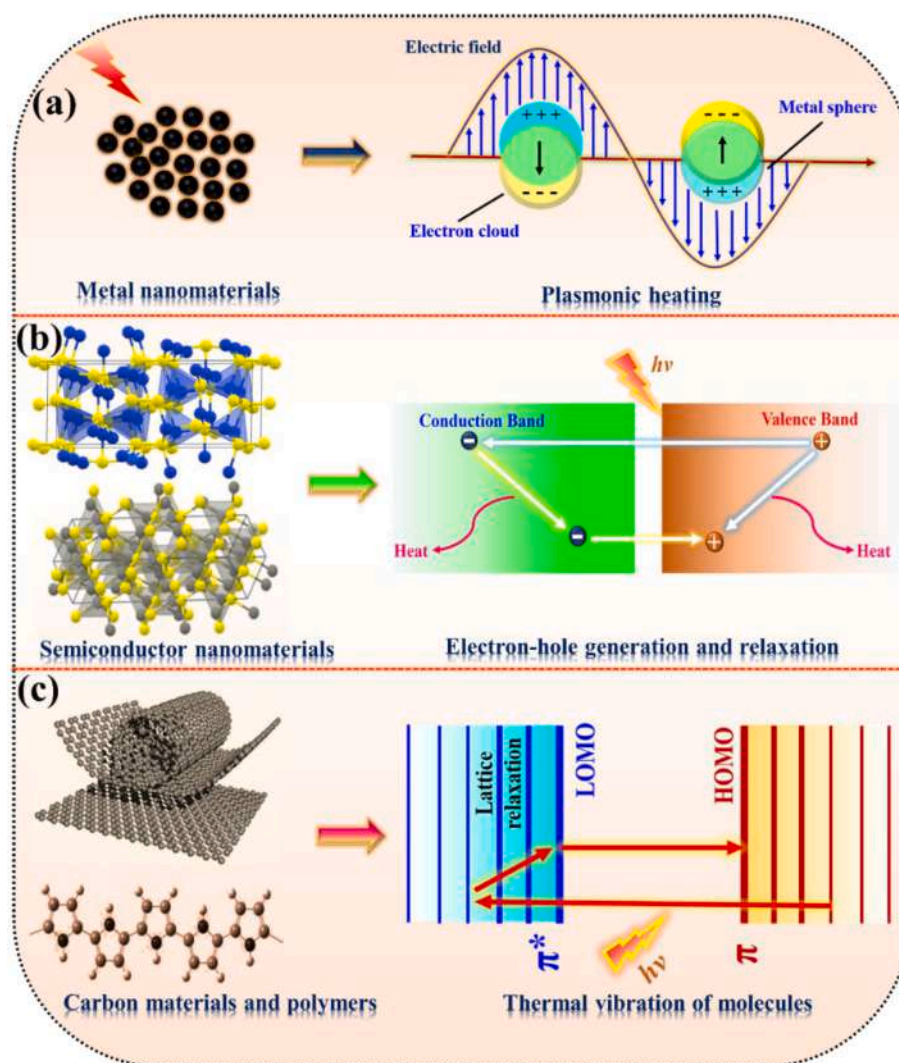
Fig. 3. Photothermal mechanisms: (a) Local metal surface plasma (b) Electron-hole generation and relaxation and (c) Thermal vibration of molecules.

Table 1
Comparison of different types of photothermal superhydrophobic materials.

Materials	Advantages	Disadvantages
Metals-based PSM	High strength	Complex fabrication
	High toughness	High production cost
	Excellent thermal stability	
Semiconductor-based PSM	Low toxicity	Limited choices
	Good stability	
	Tunable bandgap	
Carbon materials-based PSM	Broad light absorption	High production cost of graphene and CNTs
	High stability	
	Be easily made into all kinds of structures	Carbonized biomass has a fragile structure
	Widely sourced	
Polymers-based PSM	Flexibility	Limited choices
	Easy moldability	May photoage and photodegrade during use

Ag and Au nanoparticles are commonly used as photothermal conversion materials for PSM. For example, Wang et al. [28] have modified cotton surface by silver mirror reaction and thereafter by n-dodecyl mercaptan (NDM) as a hydrophobic modifier (Fig. 4a). The modified cotton has the superhydrophobic and photothermal conversion property which was effectively utilized to separate crude oil from oil-water mixture. Wang et al. [51] have prepared self-derived polymer composite sponge by Ag precursor adsorption followed the reduction of Ag^+ to Ag nanoparticles (NPs). During the reduction process the sponge was partially precipitated by Ag precursor/tetrahydrofuran (THF) and formed porous structure that improve roughness of sponge surface. The precipitation wrapped Ag NPs improved adhesiveness towards the sponge surface (Fig. 4b). The superhydrophobic, conductive and photothermal sponge demonstrated photothermal behavior and used as strain and pressure sensor. Composite sponge preserves its properties after multiple stretching, torsion, and ultrasonication treatment. Wu et al. [52] have deposited a layer of silver nanoparticles and silver nanowires (Ag NPs-Ag NWs) on the polycaprolactone (PCL)/poly (vinyl alcohol) (PVA) composite film. Thereafter deposited a layer of 1H, 1H, 2H, 2H-perfluorodecanethiol (PFDT) to attain conductive and photothermal superhydrophobic films (Fig. 4c). The underlying PCL/PVA film and Ag NPs-Ag NWs heal under low voltage or near infrared light, thus helping to recover the superhydrophobic loss due to mechanical damage caused by cuts and scratches. Tao et al. [53] have deposited the Au/TiO$_2$ composite as plasmonic photothermal material on the surface of polytetrafluoroethylene (PTFE) for photothermal superhydrophobic coating which can be utilized for defogging and deicing applications. The temperature of plasmonic photothermal film rose more than 25 °C under 300 mW/cm^2 light illumination, hence photothermal film shown outstanding deicing and anti-icing performance.

However, high costs of Ag NPs and Au NPs have limited its practical use, which prompting researchers to look for other metal nanoparticles.
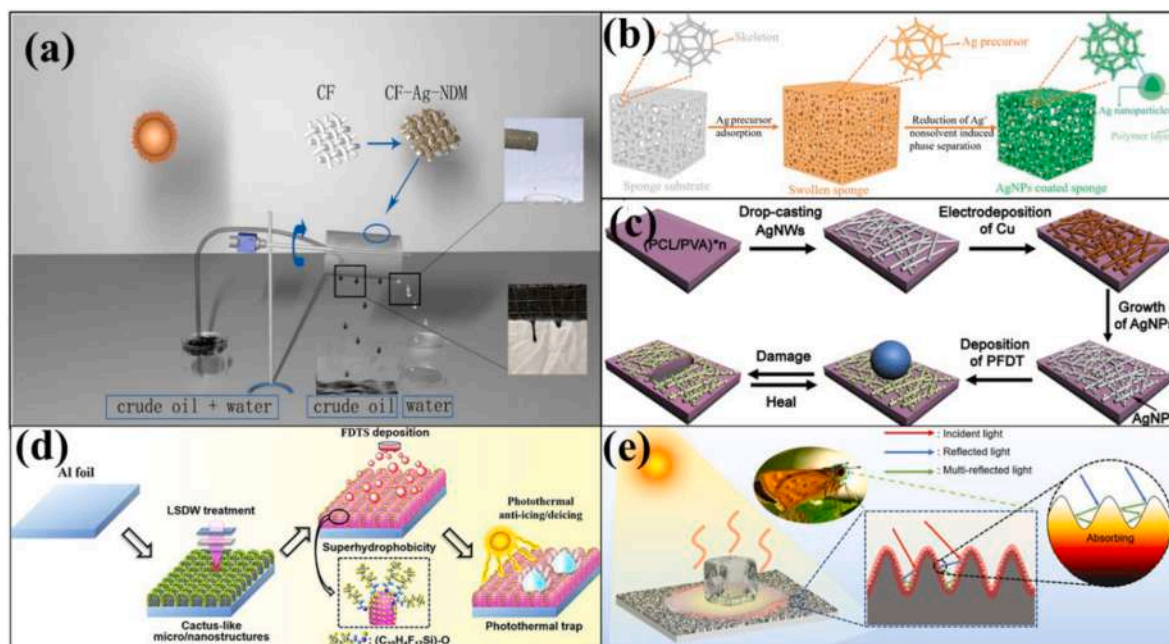
Fig. 4. (a) Preparation and application of CF-Ag-NDM [28]. (b) Photothermal superhydrophobic polymer composite sponge based on Ag NPs [51]. (c) Preparation of PFDT/Ag NPs-Ag NWs@PCL/PVA [52]. (d) Preparation of photothermal superhydrophobic Al surface [54]. (e) Schematic of MTS solar anti-icing/deicing performance [55].

Li et al. [54] have constructed black photothermal superhydrophobic Al surface by laser surface direct writing (LSDW) followed by thermal evaporation (TE) of PFDT for an anti-icing application. The constructed Al surface showed excellent superhydrophobicity with water contact angle (WCA) of 161.2° and the surface plasmonic resonance of Al micro/nanoparticles lead more than 96 % visible light-harvesting capacity (Fig. 4d). Zhao et al. [55] have created micro/nano-scaled protrusions on Al surface similar to moth eye by ultrafast laser texturing treatment and reduced its surface energy using PFDT. The hierarchical structure along with low surface energy surface has shown WCA of 162° and temperature increases up to 83 °C by absorbing 90 % of solar radiation. The hierarchical structure forms many efficient photothermal traps, which can use multiple reflections of light to gather solar energy and effectively improve the photothermal conversion efficiency (Fig. 4e). Kumar et al. [56] have sprayed composite of shellac and Cu NPs on a non-woven surgical mask (PAM). The spray coated mask shown WCA of 143° and photothermal property. Under sunlight, the surface temperature of the mask will quickly rise up to 70 °C, which will generate free radicals and reveals photocatalytic self-cleaning performance. Although PSM based on metal nanoparticles are widely prepared, the chemical instability of metal nanoparticles and the difficulty in mass production limits its practical application.

2.2. Semiconductor-based photothermal superhydrophobic materials

Semiconductor-based photothermal conversion materials (some transition metal oxides [57,58], transition metals nitrides, carbides, borides and sulfides) [59] have the advantages such as simple synthesis process, low cost, and easy to adjust the light absorption. Different semiconductors have different bandgap, which is related to the degree of light absorption. When a light is incident on semiconductor, the electron in the valence band will absorb a photon energy and jump from the valence band to the conduction band, thus creating holes in the valence band and further forming electron-hole pairs. After that, through the radiative relaxation of photons (re-radiation) or the non-radiative relaxation of phonons (heating), the energy is transferred to the surface of semiconductor, and the excited electrons lastly return to a lower band. A release of energy in the form of phonons causes local heating of

the lattice, resulting in a photothermal effect [60]. Semiconductor based PSM can be effectively prepared by using semiconductor nanoparticles to construct rough micro-nano structures or by adding low surface energy materials.

Yin et al. [61] have fabricated an inverse opal porous PDMS film with uniformly distributed Fe_3O_4 NPs by template method. The homogeneous dispersion of Fe_3O_4 NPs in the film converts the optical energy into thermal energy, affording the film with thermogenesis deicing capability in both high humidity and freezing rain conditions (Fig. 5a). Cheng et al. [62] have prepared superhydrophobic anti-icing and thermal responsive deicing coatings by depositing a composite of amino functionalized Fe_3O_4 particles and copolymer on glass/silicon substrate. A superhydrophobicity could reduce ice adhesion and efficiently prolong the freezing time. A Fe_3O_4 particles endows thermal deicing performance under sunlight (Fig. 5b). Yang et al. [63] have prepared a free-standing superhydrophobic photothermal paper by a vacuum filtration process. The mixture of synthesized ultralong hydroxyapatite nanowires and black Ti_2O_3 particles was filtered and soaked in a mixture of ethyl acetate, PDMS and curing agent. A free standing paper exhibited high flexibility and processability, high thermal stability, high photothermal conversion efficiency and stable superhydrophobicity. Ma et al. [64] have fabricated a photothermal superhydrophobic film by using titanium nitride and polytetrafluoroethylene (TiN-PTFE) for anti-icing and deicing applications. The plasmonic TiN nanorods (TiN NRs) are responsible for localized surface plasmon resonance (LSPR) performance to convert light into heat energy and low surface energy PTFE on NRs maximizes the superhydrophobicity. Xie et al. [65] have prepared photothermal icephobic copper mesh using micro silicon carbide (SiC) as photothermal conversion material and nano hydrophobic silica (SiO_2) as superhydrophobic material for anti-icing application (Fig. 5c). The coated mesh showed a WCA of 162° and a sliding angle (SA) of $3 \pm 2°$; under NIR radiation temperature of mesh rose to 35.3 °C in 220 s and rapidly melt ice layer underneath of the mesh.

Transition metal composite oxide $(CuFeMnO_4)$ has a strong absorption ability to sunlight with a wide absorption wavelength and considerable solar energy conversion efficiency [66,67]. Wang et al. [31] prepared a solar thermal coating composed of superhydrophobic SiO_2 nanospheres and $CuFeMnO_4$/PDMS. The coating has exhibited WCA of
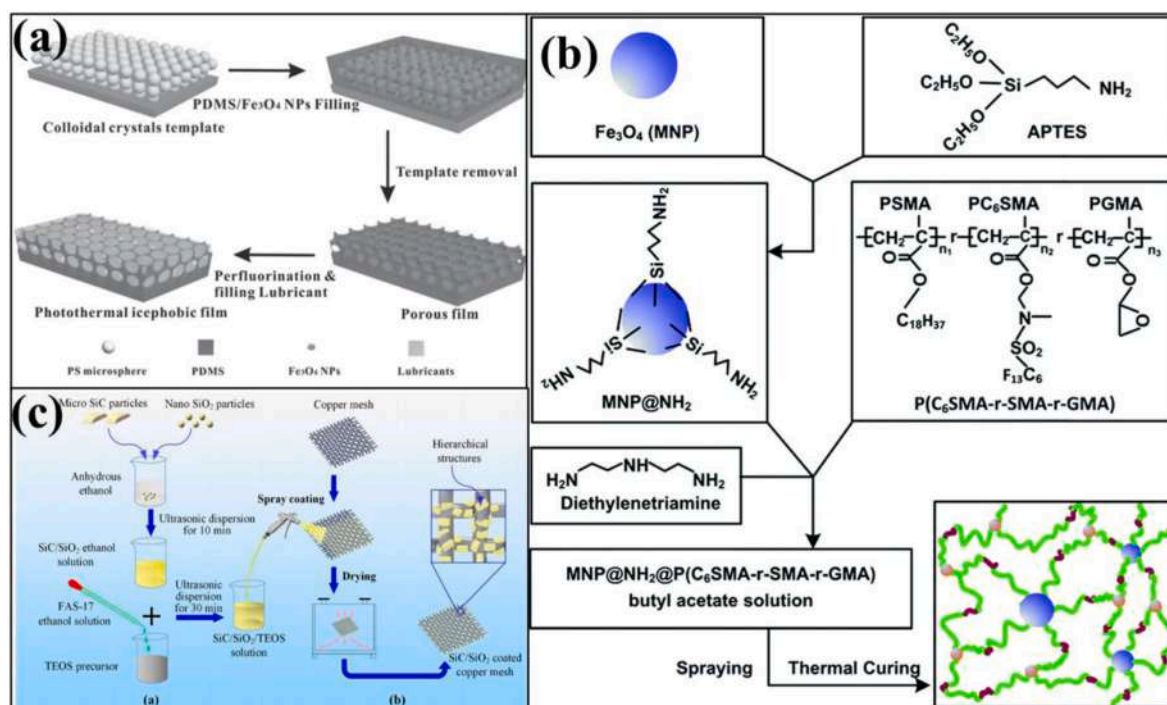
Fig. 5. (a) Fabrication of photothermal icephobic film by the template method [61]. (b) Synthesis route of MNP@NH$_2$@P(C$_6$SMA-*r*-SMA-*r*-GMA) coating [62]. (c) Preparation of SiC/SiO$_2$/TEOS solution and SiC/SiO$_2$ coated copper mesh [65].

157° and the surface temperature rose to 46.1 °C under simulated sunlight. Sun et al. [68] have synthesized a 3D macrostructure of CuFe-Se$_2$-loaded graphene aerogel (GA-CuFeSe$_2$) for photothermal conversion device. The presence of graphene provided quick diffusion of highly viscous crude oil in seawater and revealed high corrosion resistance (Fig. 6a).

MXene is a young member of the two-dimensional (2D) material family, which was first synthesized by Gogosi et al. [69]. MXene have a general formula of M$_{n+1}$X$_n$T$_x$ (n = 1, 2, or 3), where M is an early transition metal, X is carbon and/or nitrogen, and Tx represents surface functional groups (e.g. –O, –OH, and/or –F) [45,70]. MXene has attracted much attention in the preparation of PSM because of its excellent properties such as electrical conductivity, large specific surface area, high photothermal conversion efficiency (≈100 %), super-hydrophobicity, electrical conductivity and layered structure [45,71]. However, the mechanism of MXene is not fully understood at present, and many researchers are trying to uncover it. Some researchers believe that the LSPR effect leads to the photothermal conversion, and the specific mechanism needs to be further explored. Wang et al. [72] have prepared a MXene-based melamine sponge (Ti$_3$C$_2$T$_x$@MS) by hydrogen bonding between amino groups on the skeleton of MXene-based melamine sponge (MS) and polar groups on the surface of 2D MXene Ti$_3$C$_2$T$_x$ nanosheets after stripping. The sponge has a high oil absorption capacity of up to 176 times of its own weight, the surface temperature rises rapidly to 47° under light and it has shown good hydrophobicity and stability (Fig. 6b). Cao et al. [31] have applied hydrophobic 2D multi-layered/delaminated (m-Ti$_3$C$_2$Tx/d-Ti$_3$C$_2$Tx) MXene onto different substrates such as fabric, paper and glass and further modified with fluorinatedalkyl silane (FAS) to create photothermal superhydrophobic surfaces (Fig. 6c). The integrated superhydrophobicity and photothermal conversion ability displayed light-driven motion in a linear and rotational direction. Luo et al. [73] prepared a waterproof and breathable smart textile by decorating MXene on the a polydopamine (PDA) modified elastic fabric followed polydimethylsiloxane (PDMS) coating. The coated textile possesses outstanding and durable photo-thermal and electro-thermal conversion performance (Fig. 6d).

Zhang et al. [74] prepared vertically aligned MXene aerogel (VA-MXA) with upper hydrophobic layer and bottom hydrophilic layer for solar water desalination. VA-MXA has showed 87 % of photothermal conversion efficiency and stable water yield for 15 days under 1 sun.

2.3. Carbon materials-based photothermal superhydrophobic materials

Carbon material is one of the desirable materials for application of photothermal conversion, with the specific properties including high light absorption capability, considerable energy conversion efficiency, low molar specific heat, excellent mechanical and thermal stability, a wide range of applications, low cost and environmental protection. In the wide absorption range of visible light, most of the photon energy can be absorbed by electrons and take themselves in the excited state. When the excited electrons returned to the ground state, the local temperature rises and diffuses into the surrounding material. Carbon materials used for PSM are usually black because they contain a large number of conjugated double bond structures [75], and it has been reported that their layered structure is conducive to the formation of PSM. The carbon materials mainly includes carbon nanotubes (CNTs), graphene, graphite, graphene oxide (GO), reduced graphene oxide (rGO), carbon black (CB), and carbonized natural products [76,77]. Among them, CB has the advantages of wide source and low price. However, the shortcomings of CB-based PSM, such as high impurities and difficulty in controlling particle size, have prompted researchers to search for new carbon-based PSM.

Zhang et al. [78] have sprayed a composite of fluorinated polysiloxane-modified multi-walled carbon nanotubes (MWCNTs) on shape memory polymer coated magnesium alloy. Authors have reported a composite coating revealing superhydrophobic and anticorrosion property along with excellent self-healing performance under chemical and microstructure damage during sunlight irradiation (Fig. 7a and b). Xue et al. [79] have used acid chitosan to treat cotton fiber, which can make the hydroxyl group (-OH) on the fiber to form hydrogen bond with chitosan. The CNTs were applied on the fiber surface and finally, treated with PDMS for the superhydrophobicity (Fig. 7c). As-prepared fabric
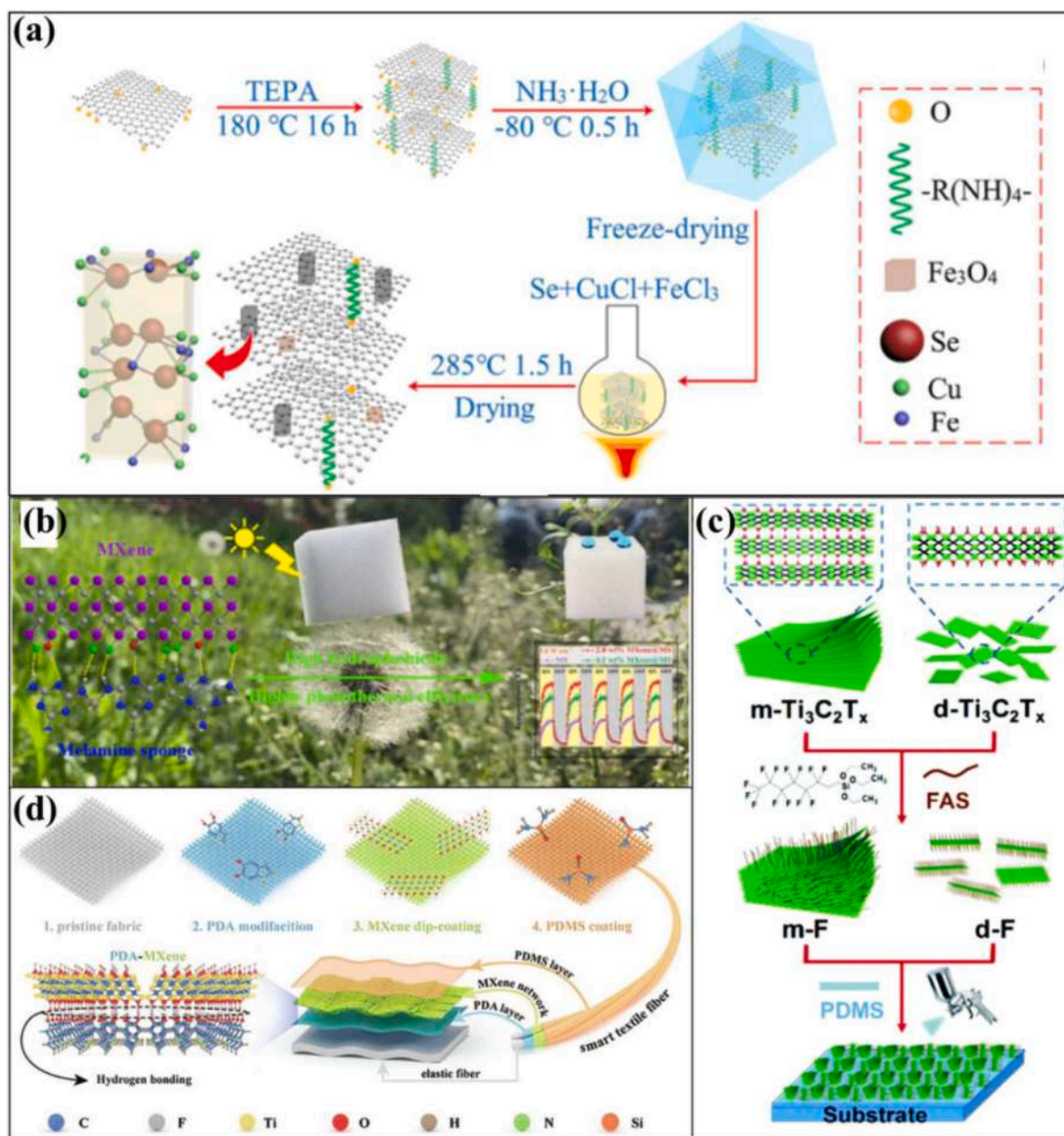
Fig. 6. (a) Synthesis of GA-CuFeSe$_2$ [68]. (b) Mxene-based melamine sponge [72]. (c) Program of hydrophobic surface fabrication using PDMS@m/d-f coating [31]. (d) Preparation of PM/PDMS textiles [73].

showed excellent photothermal conversion with 89.8 °C temperature under one sun irradiation and superhydrophobicity with CA of 165° and SA of 0.8°. Zhang et al. [25] have sprayed the dispersion of hybrid materials (CNTs-SiO$_2$) in epoxy resin on the aluminum panels using spray gun (Fig. 7d). Coated aluminum panels showed predominant superhydrophobic and photothermal conversion property and can delay the freezing time and efficiently melt the ice layer within seconds under laser irradiation. Liu et al. [80] have sprayed a nanocomposite of fluorinated multi-walled carbon nanotubes (FMWCNTs) and polyurethane (PU) on Al substrate for amphiphobic photothermal coating (Fig. 8a). Authors reported that the addition of FMWCNTs leads amphiphobic feature and high efficient photothermal conversion, which enhance deicing and defrosting characteristics under sunlight irradiation. Fu et al. [81] have demonstrated a new strategy for fabrication of porous superhydrophobic photothermal foam for removing oil spills (e.g., gasoline and diesel) from the water surface. In this process, photothermal conversion materials MWCNTs was blended in the PDMS-PU solution

and casted into the Teflon ® molds (Fig. 8b) to prepare foam capable of healing in mechanical and chemical damage and MCNTs to perform photothermal conversion. Su et al. [82] obtained the vacuum-assisted layer-by-layer superhydrophobic MWCNTs films. The film exhibited superhydrophobic feature along with electrothermal and photothermal effects (Fig. 8c). Jiang et al. [23] sprayed a suspension of silicon carbide (SiC) particles and CNTs onto the surface of ethylene-vinyl acetate (EVA) to obtain the photothermal superhydrophobic surface. Due to presence of CNTs, the coating shown light-to-heat conversion efficiency of 50.94 % in deicing tests (Fig. 8d and e).

Jiang et al. [83] have introduced laser-induced graphene coating for bacterial applications. The dual property of superhydrophobicity and photothermal conversion could reduce bacteria more than 90 % in both under solar illumination and absence of solar illumination (Fig. 9a). Wang et al. [84] have prepared photo-response superhydrophobic complex shaped microrobots using graphene/PDMS composites materials (Fig. 9b), which exhibited good superhydrophobic and
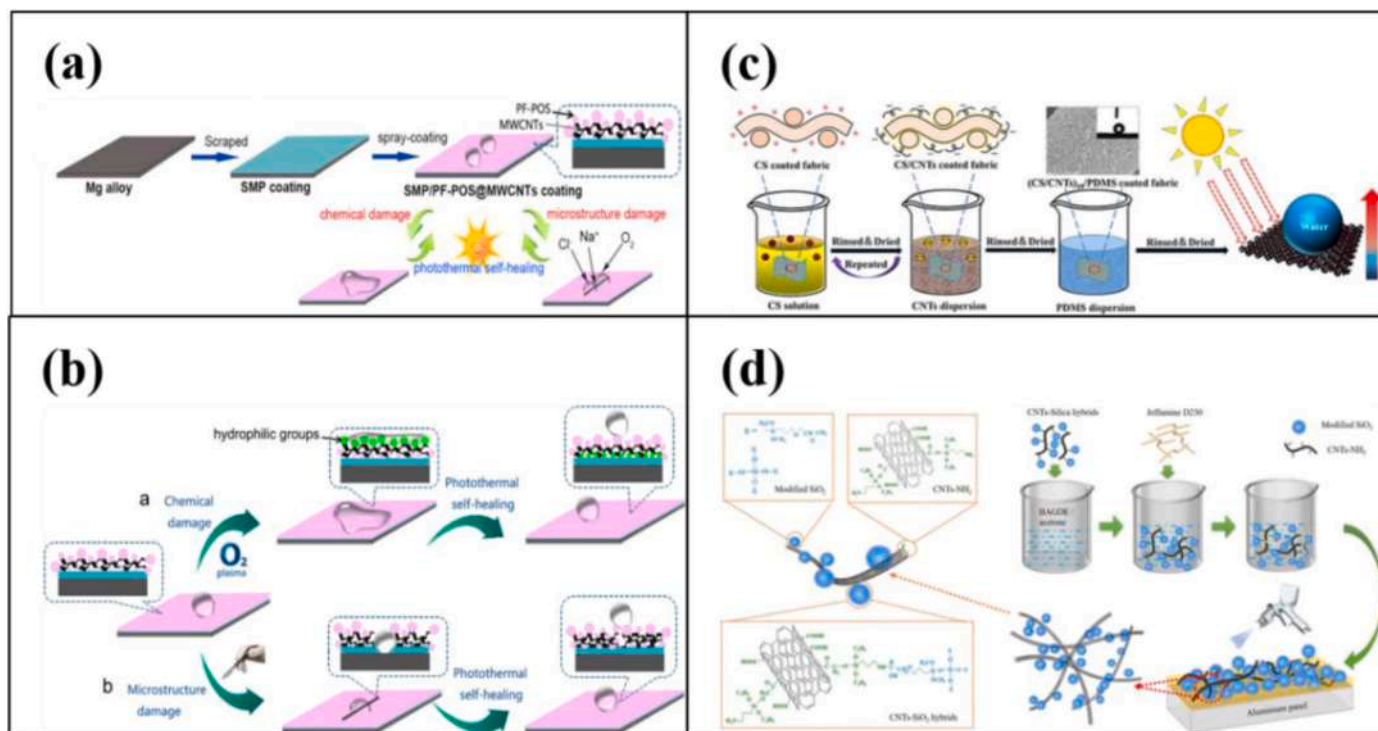
Fig. 7. (a) Preparation of SMP/PF-POS@MWCNTs coating. (b) Schematic of preparation of self-healing SMP/PF-POS@MWCNTs coatings [78]. (c) Processing technology of superhydrophobic photothermal cotton fabric [79]. (d) Synthesis of CNT-SiO$_2$ hybrid materials and superhydrophobic coatings [25].
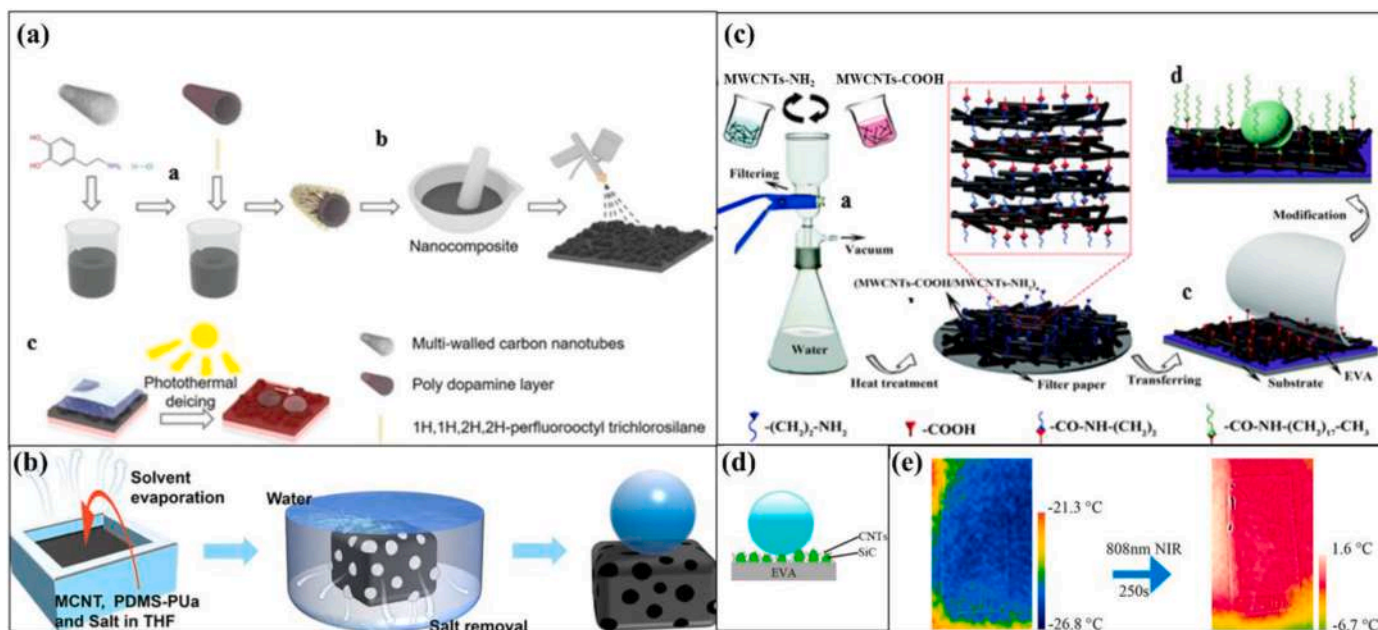

Fig. 8. (a) Schematic of preparation of photothermal amphiphilic surface: a) Fluorination of FMWCNTs; b) Photothermal amphiphilic surfaces were prepared by spraying nanocomposites containing FMWCNTs and PU prepolymers; c) Photothermal deicing performance [80]. (b) Preparation of MCNTs/PDMS-PUa foam [81]. (c) Preparation of vacuum-assisted layer by layer superhydrophobic multi-walled carbon nanotube films [82]. (d) Schematic diagram of contact model between water droplet and SiC/CNTs coating. (e) Infrared thermogram of coating surface before and after photothermal deicing [23].

photothermal properties. Zhong et al. [85] have deposited the laser-induced graphene onto commercial surgical masks for super-hydrophobic and photothermal porous coatings. Under sunlight, the surface temperature of coating increases up to 80 °C. Hence surgical masks revealed outstanding self-cleaning and photothermal properties. Zhao et al. [86] have used the condensation polymerization approach to create the stearic acid@graphene oxide/melamine-formaldehyde

superhydrophobic microencapsulated phase change materials. It showed good self-cleaning property and good photothermal conversion performance (Fig. 9c). Hu et al. [77] prepared a MOF/graphene aerogel (MEGA), which showed a WCA of 152.7°. Under light irradiation, the surface temperature of MEGA can rapidly rise to 80 °C.

Despite excellent photothermal conversion properties, the preparation of carbon nanotubes and graphene requires complex operations
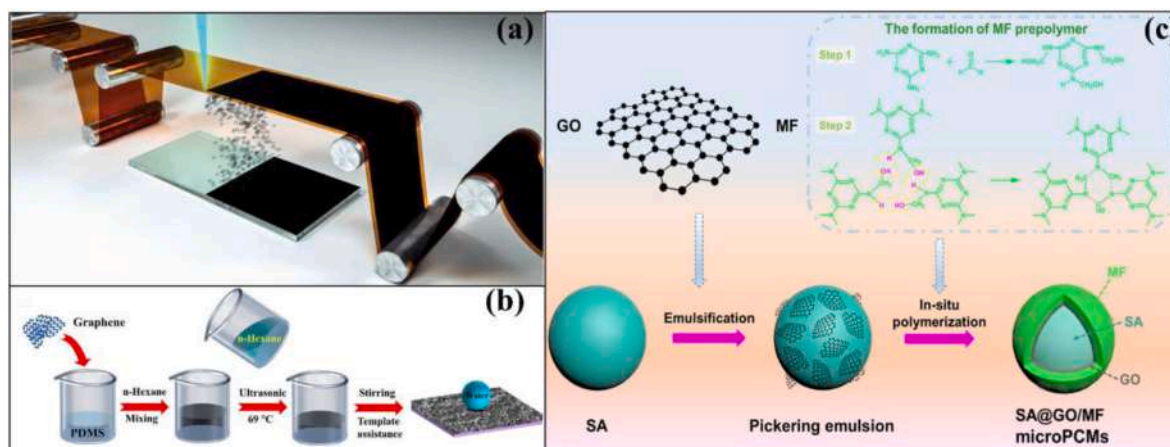
Fig. 9. (a) Schematic diagram of the process for coating graphene on glass [83]. (b) Schematic diagram of composite material preparation [84]. (c) SA@GO/MF Multifunctional miniature phase change materials synthesis schematic [86].

such as high-temperature carbonization and cracking, which increases the preparation cost of PSM. Li et al. [87] have developed a sandwich-structured photothermal wood device for moisture capture from the atmosphere. The wood pores contained the hygroscopic salt $CaCl_2$, which was sealed by hydrophobic gates constructed by PDMS and candle soot. During the absorption and desorption stages, this structure permits vapor transfer, and prevents liquid from leaving the wood (Fig. 10a). Zheng et al. [88] prepared magnetic, flexible and photothermal superhydrophobic coating by PDMS, iron powder (Fe), and candle soot (CS) (Fig. 10b). PDMS has low surface energy, Fe provides magnetic properties and CS can attain micro/nanostructures. PFe-PCS has good photothermal effect, chemical and mechanical stability.

Wu et al. [89] have deposited candle soot on glass substrate by holding it above the flame. A layer of SiO_2 shell applied on soot particles by chemical vapor deposition (CVD) of tetraethoxylsilane (TEOS). Subsequently, PDMS were grafted onto silica shells by immersing into

PDMS solution and kept under UV light (Fig. 10c). The candle soot is a core element for photothermal conversion, the silica shell improves the hierarchical strength of candle soot, and PDMS endow superhydrophobicity.

Xie et al. [90] have grown carbon nanowire arrays (CA) on carbon cloth (CC) using electrochemical deposition and followed silanization treatment (Fig. 10d). The prepared PSM's combine the blackbody properties and micro-nano hierarchical structure of carbon materials, and have excellent photothermal conversion ability and superhydrophobic property which endows excellent anti-icing performance. Kong et al. carbonized melamine foam to obtain carbonaceous materials, which not only maintained three-dimensional structure, but also had photothermal conversion performance and superhydrophobicity [91]. Some other biomass is carbonized for photothermal conversion materials due to its unique network structure, such as loofah [92], corncobs [93]. Despite the advantages of low cost, the fragile structure
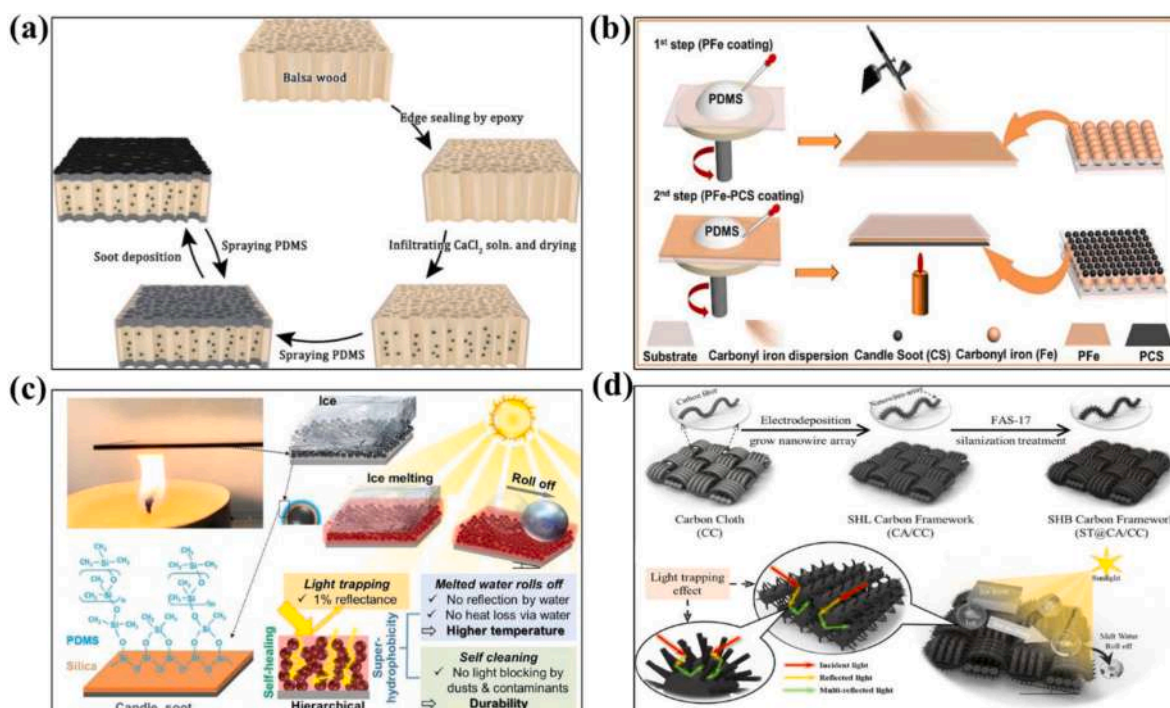
Fig. 10. (a) The production of sandwich structure photothermal wood [87]. (b) Preparation process of PFE-PCS film [88]. (c) schematic of manufacturing of superhydrophobic surface [89]. (d) Preparation and application of ST@CA/CC [90].

of carbonized biomass cannot be ignored.

2.4. Polymers-based photothermal superhydrophobic materials

Similar to carbon materials, polymers such as polydopamine (PDA), polyaniline (PANI), and polypyrrole (PPy) [94] have a photothermal conversion mechanism that depends on molecular thermal vibration. Conjugated polymers usually composed of highly π-conjugated polymeric backbones bearing contiguous sp^2-hybridized carbon atoms, with the advantages of high light absorption, excellent flexibility, easy forming, and long-term biocompatibility. Compared to other types of PSM, the unique flexibility of polymer-based PSM makes it suitable for a variety of substrates and application environments. However, some polymer-based PSM may photoage and photodegrade during use, which limits the durability of the material and the stability of use.

The main chain of PANI contains a large number of imino and imine nitrogen atoms, which is beneficial to the wettability control of the material surface. Li et al. [95] have modified MS using a PDMS/PANI by simple polymerization and dip-coating. The unique PANI coating endows superior photothermal conversion efficiency with temperature rose to 81.8 °C within 2 min under 1 kW/m^2 sunlight (Fig. 11a). PPy can be directly polymerized on various substrates to form PSM micro and nano structures. Wu et al. [96] have fabricated photothermal composite membrane by depositing polypyrrole nanotubes (PPy NTs) coating layer onto an electrospun PVDF nanofibrous by vacuum filtration method. The PDMS was used as an adhesive to enhance the adhesion between the PPy layer and the PVDF substrate. Membrane exhibits high photothermal conversion efficiency of 81.6 % with superhydrophobic characteristic (Fig. 11b).

With the continuous development of research, PSM based on different types of photothermal conversion materials have been deeply studied. Compared with precious metal nanoparticles, semiconductor materials and carbon materials show better application prospects because of their advantages of low cost, easy preparation, and rich variety. In recent years, researchers have noticed that the composite of different types of photothermal conversion materials may enhance their solar absorption and photothermal conversion capabilities, which is beneficial for the improvement of the performance of PSM [50,97]. For example, the composite of semiconductor and carbon material, organic and semiconductor material. He et al. prepared PDA/FeCo$_2$S$_4$/PDMS@PU by attaching PDA and FeCo$_2$S$_4$ to PU sponge successively. Thanks to the collaborative photothermal conversion capability of PDA and FeCo$_2$S$_4$, the PDA/FeCo$_2$S$_4$/PDMS@PU displays wide absorption in the wavelength range of 300 nm–2000 nm, and the surface temperature can reach 74.8 °C under 1 standard sunlight [98]. In the future research, the stability of the composite and the control of reactant ratio to obtain higher photothermal conversion performance are to be obtained.

3. Photothermal superhydrophobic materials: sustainable applications

3.1. Sea water desalination

The lack of fresh water is a major problem for nearly one - third of the world's population [99]. Since the earth is rich in sea water resources, obtaining fresh water from sea water by desalination is considered to be an effective way to solve the crisis of water shortage. Traditional desalination technologies (membrane distillation (MD), reverse osmosis (RO), electrodialysis) necessitate complex equipment, high costs and high energy consumption, which severely limits their widespread use [100,101]. In recent years, solar interfacial evaporation has attracted much attention due to its advantages of cheap, eco-friendly, and green solar energy consumption [102–107]. In this technology, photothermal evaporator absorb solar radiation and convert it into heat at surface of water and evaporator, water steam to be generated. However, the poor salt scale and stability in the long-term solar desalination process seriously hinder the application of the solar evaporator. The salt resistance strategies of the surface of the photothermal interface evaporator are mainly divided into two categories: "salt-out" and "salt-free". The "salt-out" strategy mainly includes physical cleaning, local crystallization and gravity-assisted cleaning. The implementation cost of this method is high and the cycle is long. Besides, during the crystallization process, the salt covers the surface of the evaporator, resulting in the reduction of evaporation rate. The "salt-free" strategy mainly includes ion exclusion, surface hydrophobic modification, non-contact evaporation, and reverse diffusion/convection. As a widely used salt resistance strategy, hydrophobic surface modification is a way to confine high salinity ions to the hydrophilic layer through heterogeneous wettability, which is conducive to rapid dissolution.

In Table 2, the currently reported studies on PSM for seawater desalination application were represented. Evaporation rate is a key parameter to measure the water evaporation performance of PSM. At present, the evaporation rate of PSM evaporators prepared in most literatures is between 1 and 3 kg m^{-2} h^{-1}. Researchers are working to get higher evaporation rates via changing photothermal conversion materials and optimizing devices. For example, Tian et al. [108] designed a three-dimensional cylindrical evaporator based on Ag–MnO$_2$ and graphene aerogel, and obtained a solar evaporation efficiency of 6.46 kg m^{-2} h^{-1} under a standard sunlight. In future research, new photothermal materials and photothermal evaporation devices with special designing need to be prepared to reduce heat loss and obtain higher evaporation rate.

3.2. Passive anti-icing/active deicing

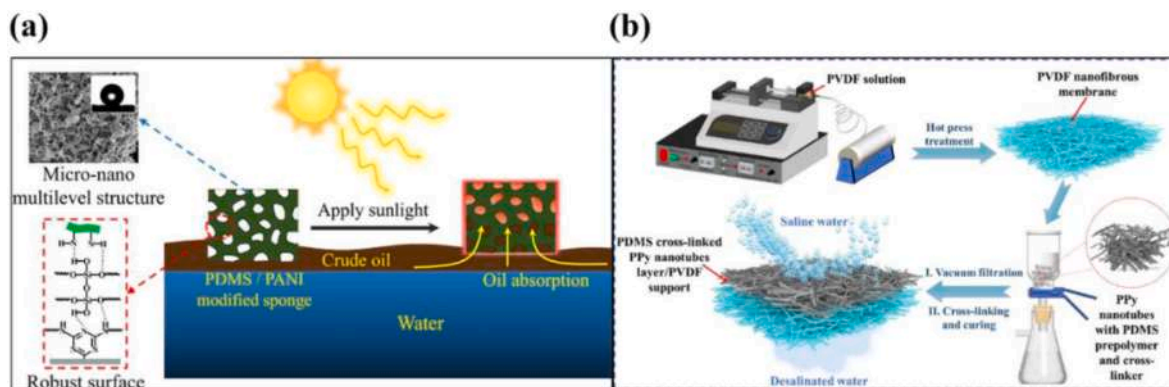The ice accumulation has irretrievable losses and catastrophic affairs

Fig. 11. (a) Preparation and application of PDMS/PANI@MS [95]. (b) Schematic diagram of PPy NTS/PVDF superhydrophobic composite membrane preparation [96].

Table 2

Reports on PSM for seawater desalination.

Materials	Method	WCA (°)	Photothermal conversion performance			Evaporation rate (kg·m^{-2} h^{-1})	Ref.
			Power intensity (W/ m^2)	Absorption (%)	T (°C)		
VA-MXA	Template method	133.2	600	96	59	1.46	[66]
PDMS/CNTs/PVDF	Spray-coating	146.6	1000	/	70	1.43	[101]
S-CPM	Spray-coating	150.8	1000	91	41	1.41	[99]
CNT−SiO$_2$ Bilayered Material	Sol-gel	142.0	1000	/	72	1.31	[109]
BCP$_n$	Spray-coating	159.5	1000	/	82	1.31	[110]
Mx@SPF	Spray-coating	160.0	1000	/	55	1.22	[111]
PPy/PFDTS@fabric	Dip-coating	160.4	1000	98	67	1.49	[112]
PDMS/CNTs@MS	Spray-coating	147.8	1000	99	96	1.44	[103]
PDMS@Ink@Fabric	Dip-coating	156.2	1000	/	50	0.49	[113]
PPy/PVDF Membrane	Template method	114.0	1000	/	70	1.42	[114]
PDMS/ink/TiO$_2$@MS	Spray-coating	126.5	1000	97	40	1.49	[115]
Ti$_3$C$_2$T$_x$/O-CNTs@PU membrane	Chemical cross-linking and vacuum filtration	130.2	1000	/	50	1.66	[116]
Ti$_4$O$_7$/YSZ nanofiber	Electrospinning	/	1000 and 3V voltage	/	75	7.51	[117]
h-BN/PPy@MF	Dip-coating	147.3	1000	/	51	1.21	[118]
Co@C/NCNT@nylon membrane	Vacuum filtration	128.5	3000	/	60	1.55	[119]
MN-PCG	Micro extrusion compression molding technology	156.0	1000	/	96	2.42	[120]
Janus P(AM-DMDAAC)/GO aerogels	Freeze-dried	133.6	1000	/	77	3.65	[121]

[VA-MXA: vertically aligned Janus MXene aerogel; S-CPM: CNT@PVP membrane; BCPn: a tetrahydrofuran (THF) dispersion of the beeswax, MCNTs, PDMS base, and PDMS curing agent was layer-by-layer sprayed onto the substrates to obtain the porous and rough BCPn coatings (where n is the number of spraying cycles); Mx@SPF: x is the number of repetitions, M represents MXene, S and P represent SiO$_2$ and PDMS, F represents the PFOTES; O-CNTs: oxidized carbon nanotubes; YSZ: yttria-stabilized zirconia; h-BN: boron nitride; MN-PCG: micro/nanostructured polyethylene/carbon nanotubes foam with interconnected open-cell structure.].

in various residential activities and industries, transport systems, energy equipment and telecommunications system [66]. Over the past few decades, many deicing strategies, such as electro-thermal or steam-heated melting, de-icing chemicals and mechanical vibrations have been utilized to remove accumulated ice on cold surfaces (for example, aircraft wings, ship decks and wind turbine blades). Such type of deicing method is also called active deicing, which requires

mechanical removal, chemical and thermal technology, and has some disadvantages such as low efficiency, poor mechanical stability, difficult operation and produces secondary pollutants [122,123]. Passive anti-icing, by contrast, does not require external energy to prevent ice accumulation and has the advantages of being environmentally friendly and cheap.

PSM can realize the combination of passive anti-icing and active de-

Table 3

Reports on PSM for passive deicing and anti-icing.

Materials	Method	WCA (°)	Photothermal conversion		t1 (s)	t2 (s)	Adhesion strength (KPa)	Ref.
			T (°C)	Power intensity (W/ m^2)				
SiC/CNTs@EVA	Spray-coating	161.0	173	/	66	250 (−30 °C)	25.7–2.7	[23]
ODA-MWCNTs-COOH/NH$_2$)n@EVA	LbL	165.0	71	/	/	/	/	[82]
TiN-PTFE NPs@Q235 steel	Deposition	156.0	60	20000	78	50 (−10 °C)	/	[68]
SiO$_2$/SiC@EVA	Spray coating	162.0	200	25000	326	28 (−30 °C)	52.2–4.4	[123]
PVDF/CNTs@GS	Spray coating	163.0	40	1000	58	296	16.8–13.2	[24]
F–Fe$_3$O$_4$ NPs@Al	Inverse infiltration	161.0	/	/	2100	60 (−10 °C)	/	[124]
CS/SiO$_2$/PDMS@GS	CVD	163.0	53	1000	/	300 (−50 °C)	/	[89]
CA@CC	Electrochemical deposition	155.0	90	1000	3600	94 (−15 °C)	/	[90]
melanin/F–SiO$_2$@GS	Spray-coating	160.3	68	1000	144	600 (−20 °C)	104.1–25.7	[126]
MWCNTs-PEG400DA xerogel	Template method	155.0	39	1000	2040	1560 (−30 °C)	/	[127]
CNTs-SiO$_2$@Al	Spray-coating	159.3	80	10000	165	60 (−20 °C)	/	[25]
PPy/ATP@hexadecylPOS@Al	Spray-coating	162.7	70	1000	600	180 (−10 °C)	789.2–51.6	[94]
PDMS/Fe/CS@GS	Spray-coating	154.5	94	1500	385	237 (−20 °C)	/	[88]
Fe$_3$O$_4$@AAO	Vacuum impregnation	122.0	45	/	/	30	57.8–0.2	[128]
SiC/SiO$_2$@copper mesh	Spray-coating	162.0	48	1000	82	300 (−30 °C)	5.9–1.7	[69]
CuFeMnO$_4$/PDMS@Al	Spray-coating	157.0	46	1000	91	99 (−35 °C)	1230.0–12.1	[71]
Fe$_3$O$_4$/SiO$_2$/HMDS@Fabric	Spray-coating	150.0	53	/		40 s	/	[129]
PMHS//NiP/PET@Fabric	Spray-coating	141.2	72	1000	1018	455 (−10 °C)	135.0–55.1	[130]
CNP@PDMS	Salt-template	153.5	75	1000	648	129 (−20 °C)	79.4–0	[131]
FBC/TiN@filter	Dip-coating	159.2	63	1000	831	55 (−20 °C)	/	[132]
GOF@PVDF	Phase separation	154.0	72	1000	213	/	153.5–59.7	[133]
PMTFPS/CNTs@ tinplate sheet	Spray-coating	160.8	49	/	152	/	420–33.3	[134]

[t$_1$: icing delaytime; t$_2$: icing melting time; EVA: ethylene vinyl acetate; ODA: n-octadecylamine; LbL: Layer-by-layer deposition; GS: Glass slides; CA: carbon-nanowire array; PED400DA: Polyethylene glycol diacrylate; AAO: anodic aluminum oxide; HDMS: 1, 1, 1, 3, 3, 3-hexamethyl disilazane; PMHS: Polydimethylhydrosiloxane; CNP: Carbon nanopowde; FBC: fluorinated biochar; PMTFPS: poly (methyl-3,3,3-trifluoropropyl siloxane)].

icing, which can effectively reduce energy consumption and improve the anti-icing/de-icing efficiency of the coating [69,123]. On the one hand, the hydrophobic nanoscale/differential layer structure can firmly trap air in the surface texture and minimize the effective water-solid contact area, so that the surface of PSM cannot be wetted by the water droplets in Cassie state with large CA and small SA. On the other hand, photo-thermal conversion materials absorb inexhaustible solar energy to generate heat, which can accelerate the melting of ice on the surface of the material and reduce the accumulation of ice [123–125]. In Table 3, the currently reported studies on PSM for passive deicing and anti-icing application were represented. In future, problems such as loss of hy-drophobicity and poor durability of PSM used for deicing/anti-icing need to be solved.

3.3. Crude oil cleaning

Petroleum is an important natural resource, which is mainly composed of alkanes, cycloalkanes and toluene. In the process of exploration, production and transportation, oil spill and random discharge of oily wastewater occur from time to time, which pose a serious threat to the ecological environment and human health [135]. About 120 million gallons of crude oil and its refined products leak into the environment globally every year [136]. Traditional filter-ing/adsorption methods, such as physical method (centrifugation, skimming, gravity separation and coagulation-flocculation) and chem-ical method, usually show the disadvantages of low efficiency, heavy equipment, complex operation and damage to the environment, which limits their practical application [137,138].

The hydrophobic and oleophilic adsorption materials are often used to absorb oil with the advantages of low cost and flexible operation. Common adsorption materials are foam, melamine sponge (MS), poly-urethane sponge (PU) and cotton. In recent years, porous materials such as Metal–organic frameworks (MOFs) [139–141] and aerogel [142–144] have also been used to separate oil from water. However, it is only suitable for the recovery of low viscosity crude oil. Especially when the oil leaked into the atmosphere is exposed to sunlight, it will be converted into viscous crude oil through evaporation and natural photo-oxidation. PSM has excellent solar heating performance, thus reducing the viscosity

of surrounding crude oil (the higher the temperature, the lower the viscosity of crude oil), improving the flow of crude oil, and achieving higher separation efficiency, which has attracted more and more attention [145,146]. Table 4, represents the currently reported studies on PSM for crude oil cleaning. However, it is difficult to compare these oil-water separation performances of different materials due to the different types of oil used in the oil-water separation experiment and the different measurement conditions.

3.4. Photothermal disinfection

The emergence of COVID-19 in 2019 had a great impact on more than 210 countries and regions in the world [85]. As an important strategy to prevent the spread of respiratory viruses, masks can effec-tively reduce the risk of infection. Existing masks (N95) have a hydro-phobic surface. However, the process and decontamination of masks is challenging and high risk [56,85]. Due to the limited cleaning capacity, water droplets containing the virus may remain on the mask. At the same time, the difficulty of recycling used masks causes great economic costs and environmental impacts. Chemical and thermal decontamina-tion are common decontamination methods [159]. In contrast to chemical decontamination, which may break down polypropylene fi-bers, thermal decontamination does not destroy the integrity of the mask. PSM is a widely used and promising decontamination material owing to the advantages of highly water repellent, quickly heating under solar illumination and fast and low cost production. Table 5, represents the currently reported studies on PSM on mask.

3.5. Photothermal actuation

Stimulus-responsive actuators, a kind of machine that responds to external stimuli and converts external energy into dynamic motion behavior are promising for applications in robotics, micro-generators, environmental remediation and biomedical engineering. Researchers have used various strategies to achieve stimulus-responsive actuation, such as vapor enabled propulsion, Marangoni effect and magnetically powered motion. Among the above methods, the Marangoni effect is considered an attractive option due to the advantages of environmental,

Table 4
Reports on photothermal superhydrophobic coatings for crude oil cleaning application.

Materials	Method	WCA (°)	Photothermal property		Solar-assisted absorption		Ref.
			Power intensity (W/m^2)	T (°C)	Viscosity (mPa·s)	Absorption capacity	
PDA/PDMS@MS	Deposition	134.0	1500	79	10^4–10.0	1.3×10^6 g/m^3	[29]
Fe$_3$O$_4$/PDMS@MF	Dip-coating	158.0	1000	71	5.3×10^3–1.0×10^2	42.0 g/g	[147]
PDMS/PANI@MS	Dip-coating	154.0	1000	82	1.2×10^4–26	11.7×10^5 g/m^3	[95]
rGO/AgNPs@MS	Dip-coating	130.0	1000	67	2.1×10^4–10.0	68.0 g/g	[146]
PDMS/CuS/PDA@MS	Deposition	169.3	1000	87	4.3×10^4–52.0	117.0 g/g	[27]
Ti$_3$C$_2$T$_x$@MS	Dip-coating	150.0	10000	47	/	/	[64]
Ag/NDM@CF	Silver mirror reaction	155.0	1000	70	1.1×10^3–20.0	/	[28]
carbonized MS	Carbonization	152.0	600	75	/	76.1–192.1 g/g	[91]
CNT@PU	Dip-coating	154.0	1200	88	1.1×10^5–1.6×10^3	188.0 g m^{-2} min $^{-1}$	[148]
PPy/PEG/PODS@MS	Dip-coating	120.0	/	45	1.0×10^3–5.5×10^2	29.2 g/g	[138]
rGO@MF	Dip-coating	141.0	1000	89	/	/	[136]
OTS/rGO@WS	Dip-coating	134.2	1000	88	/	7.3g/g-0.8 g/cm^3	[145]
CNT/rGO aerogels	CVD	140.5	1000	83	8.5×10^4–1.5×10^3	267.0 g/g	[149]
m-CNT/PPy@MS	In situ polymerization	158.0	1000	119	6.1×10^4–3.6×10^2	6.1 kg/m^2	[150]
PDMS/CNFs@PDMS	Template method	151.0	1000	76	1.34×10^4–253	/	[151]
Fe$_3$O$_4$/SiO$_2$/HMDS@PU	Spray-coating	150.0	/	/	/	> 15 g/g	[129]
PDMS/Fe$_3$O$_4$/PPy@MS	Dip-coating	155.0	1000	96	/	/	[152]
PDMS/CuS/CFs/rGO sponge	/	/	300	76	3.0×10^5–108.6	66.8 g/g	[153]
PDMS/MPfFn/PPy@MS	Dip-coating	148.0	1000	82	6.2×10^4–97.4	25.6 g/g	[154]
MoS$_2$/PDMS/MS	Dip-coating	151.8	1000	60	/	77.6 g/g	[155]
PVDF/SiO$_2$@GO aerogel	Electrospinning and freeze drying	143.7	1000	70	/	129.0–264.0 g/g	[156]
PFS@GC@PDMS	/	141.0	1000	68	1.8×10^4–3.7×10^2	12.0–27.8 g/g	[157]
rGO/CNTs@MS	LbL	151.0	1000	75	/	1.7 g/cm^2	[158]

[MS: melamine sponge; MF: melamine-formaldehyde; rGO: reduced graphene oxide; NDM: n-dodecyl mercaptan; CF: cotton yarn; PEG: npolyethylene glycol; PODS: polymerized octadecylsiloxane; WS: wood sponge; OTS: octadecyltrichlorosilane; CNFs: Carbon nanofibers; MPfFn: magnetoferritin nanoparticles.].

Table 5

Reports of PSM on mask.

Materials	Method	WCA (°)	Photothermal property			Ref.
			Power intensity (W/m^2)	Absorption (%)	T (°C)	
GO@mask	Laser-induced	141.0	1000	95	80	[85]
Ag/GO@mask	Laser-induced	140.0	1000	95	80	[159]
shellac/CuNPs@mask	Spray-coating	143.0	2000	99	70	[56]
CNTs@mask	Spray-coating	156.2	1000	/	90	[160]
GO@mask	laser-induced	150.0	750	/	52	[161]
Cu$_{2-x}$S@mask	Dip-coating	106.0	500	/	78	[162]

efficient and cheap [163]. In the Marangoni effect, the liquid with relatively small surface tension flows along the gradient of tension to the liquid with larger surface tension, thus driving the movement of the device [163]. Superhydrophobicity and excellent photothermal conversion efficiency are important factors affecting Marangoni flow [164].

Many efforts have been reported PSM are successfully used for light-driven self-propelled motion [31,82]. Yang et al. [163] prepared a superhydrophobic photothermal paper based on ultralong hydroxyapatite nanowires. The paper can absorb energy and convert it into heat, which is used for self-propelled motion driven by optical light with controllable motion direction and speed. Song et al. [164] prepared carbon nanofiber (CNF) hybrid membrane using polyacrylonitrile and nickel acetylacetonate as raw materials. When exposed to near infrared (NIR) laser irradiation, the CNF hybrid membrane temperature can rise to 102.1 °C in 25 s, triggering the Marangoni effect. The linear and rotational motion of the hybrid membrane can be realized by reducing the motion resistance. Wang et al. [84] prepared graphene/polydimethylsiloxane composites. A robot with infrared driving performance is developed using composite materials, which can realize linear, rotary and oscillatory motion at the air/water interface. Wu et al. [165] prepared superhydrophobic coating by spraying fluorinated acidified carbon nanotubes and Fe$_3$O$_4$/PDMS on filter paper. Under one sun irradiation, the temperature of the surface of the paper rises to 130 °C and the optical drive motion based on the Marangoni effect can be achieved (Fig. 12).

4. Conclusions and outlooks

PSM revitalize energy-intensive applications in place of traditional energy utilization. In this review, the fundamental of wetting structures and the role of photothermal nanomaterial in the construction of hierarchical surface structure were thoroughly discussed. The combined effect of superhydrophobic and photothermal conversion has been highlighted which extended the range of PSM applications. Metal, semiconductors, carbon/carbon derivatives, and polymers are the main component of photothermal conversion materials. Along with photothermal nanomaterial's, the low surface energy materials, such as various polymers, PDMS and siloxanes are used to increase the hydrophobicity of the coating surface. The current state of development of PSM, as well as their potential applications on different industrial scales has been comprehensively reviewed. Extensive research progress has been realized with the innovation in nanotechnology and advanced applications in response to researcher's demands.

Despite above, researchers are facing some crucial obstacles in fabricating PSM for viable applications. Several challenges and suggestions are outlined, which are expected to be helpful for future research.

1) Researchers are working on the preparation of photothermal materials with extremely high absorption rates. It should be noted that the low cost, large-scale preparation, environmental compatibility, flexibility and long-term stable photothermal conversion performance of photothermal materials are crucial for the application of PSM in daily life. In addition, it is necessary to develop temperature
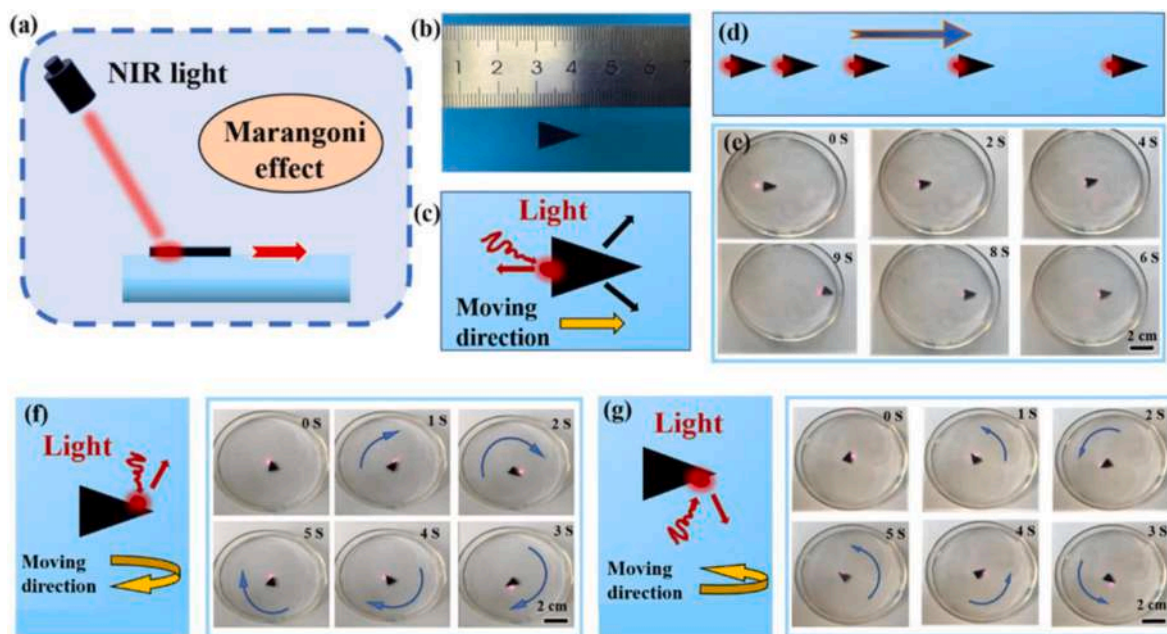
Fig. 12. (a) Schematic description of the object movement induced by the Marangoni effect. (b) The triangle shape of the FCIP@paper designed for motion. (c) Force analysis of the FCIP@paper for the linear forward propulsion. (d) Schematic demonstration and (e) photograph of the linear motion. Force analysis and photographs of the FCIP@paper for (f) clockwise and (g) anticlockwise rotational motion [165].

control research for the surface of photothermal materials, as different applications have different temperature requirements.

2) The methods used for the preparation of PSM, such as etching method and sol-gel method, may have shortcomings such as high equipment requirements and cumbersome operation steps, which limit its practical application. In future, the design of simple, efficient and low-cost methods is an important research direction.

3) In hydrophobic modification, the use of fluorine-containing reagents may have a negative impact on the human body and the environment, which makes researchers look for new hydrophobic modification materials to replace the fluorinated hydrophobic modification agents.

4) The long-term stability of PSM can guarantee its service life in practical applications. However, PSM can be scraped or broken down, which limits long-term sustainable applications. The preparation methods of PSM with high stability mainly include the design of reasonable structure, the construction of chemical bonding, the strengthening of the interface between hydrophobic material and substrate, and the endorsing of PSM with self-healing properties. In future studies, one or a combination of the above methods can be used to explore PSM with beneficial mechanical properties and stability. At the same time, reliable methods for evaluating the mechanical durability of PSM must be developed.

5) Due to differences in experimental methods, measurement techniques and data processing, there are no unified standards to evaluate the potential of various PSM in practical applications. For example, it is difficult to assess the water evaporation performance of different PSM. Therefore, it is particularly important to establish a uniform evaluation method (measurement conditions, calculation methods) to make the comparison of different materials more intuitive.

6) Different PSM-based evaporation devices have been used for solar desalination, reducing heat loss and significantly increasing the evaporation rate of water. In subsequent studies, factors such as latent heat and environmental energy should be considered. In addition, some volatile organic compounds may be collected with water during evaporation, leading to secondary pollution, which can be solved by developing multifunctional materials with photothermal superhydrophobicity and the ability to remove volatile organic compounds.

In summary, PSM has been widely used in many application scenarios due to its excellent photothermal conversion and superhydrophobic properties. In future work, it is hoped that researchers can explore new methods to improve the photothermal conversion performance and stability of PSM, so as to further expand its application range.

Author contributions

Sijie Cheng Investigation, Writing – original draft, Writing – review & editing; Sanjay S. Latthe Investigation; Kazuya Nakata Investigation; Ruimin Xing Conceptualization, Funding acquisition, Project administration, Supervision,; Shanhu Liu Conceptualization, Funding acquisition, Investigation, Project administration, Supervision, Writing – review & editing; Akira Fujishima Investigation and Supervision.

Declaration of competing interest

The authors have no conflicts of interest to declare that are relevant to the content of this article.

Data availability

Data will be made available on request.

Acknowledgements

References

[1] B. Yang, C. Li, Z. Wang, Q. Dai, Thermoplasmonics in solar energy conversion: materials, nanostructured designs, and applications, Adv. Mater. 34 (26) (2022), e2107351.

[2] S. Mekhilef, R. Saidur, A. Safari, A review on solar energy use in industries, Renew. Sust. Energ. Rev. 15 (4) (2011) 1777–1790.

[3] E. Romero, V.I. Novoderezhkin, R. van Grondelle, Quantum design of photosynthesis for bio-inspired solar-energy conversion, Nature 543 (7645) (2017) 355–365.

[4] D. Zhang, Y. Ren, X. Fan, J. Zhai, L. Jiang, Photoassisted salt-concentration-biased electricity generation using cation-selective porphyrin-based nanochannels membrane, Nano Energy 76 (2020), 105086.

[5] Z. Chen, Y. Lin, Q. Qian, P. Su, Y. Ding, P.D. Tuan, L. Chen, D. Feng, Picosecond laser treated aluminium surface for photothermal seawater desalination, Desalination 528 (2022), 115561.

[6] G. Jiang, Z. Liu, J. Hu, Superhydrophobic and photothermal PVDF/CNTs durable composite coatings for passive anti-icing/active de-icing, Adv. Mater. Interfaces 9 (2) (2022), 2101704.

[7] X.D. Liu, B. Chen, G.G. Wang, S. Ma, L. Cheng, W. Liu, L. Zhou, Q.Q. Wang, Controlled growth of hierarchical Bi$_2$Se$_3$/CdSe-Au nanorods with optimized photothermal conversion and demonstrations in photothermal therapy, Adv. Funct. Mater. 31 (43) (2021), 2104424.

[8] Z. Fang, S. Jiao, Y. Kang, G. Pang, S. Feng, Photothermal conversion of W$_{18}$O$_{49}$ with a tunable oxidation state, ChemistryOpen 6 (2) (2017) 261–265.

[9] Y. Liu, Y. Zhou, Y. Lin, G. Jia, One-pot microwave-assisted synthesis of Ag$_2$Se and photothermal conversion, Results Phys. 38 (2022), 105590.

[10] W. Barthlott, C. Neinhuis, Purity of the sacred lotus, or escape from contamination in biological surfaces, Planta 202 (1) (1997) 1–8.

[11] W. Zhang, D. Wang, Z. Sun, J. Song, X. Deng, Robust superhydrophobicity: mechanisms and strategies, Chem. Soc. Rev. 50 (6) (2021) 4031–4061.

[12] X. Zhang, F. Shi, J. Niu, J. Jiang, Z. Wang, Superhydrophobic surfaces: from structural control to functional application, J. Mater. Chem. 18 (6) (2008) 621–633.

[13] K. Senthil, G. Kwak, K. Yong, Fabrication of superhydrophobic vanadium pentoxide nanowires surface by chemical modification, Appl. Surf. Sci. 258 (19) (2012) 7455–7459.

[14] P. Dimitrakellis, E. Gogolides, Hydrophobic and superhydrophobic surfaces fabricated using atmospheric pressure cold plasma technology: a review, Adv. Colloid Interface Sci. 254 (2018) 1–21.

[15] A. Elzaabalawy, S.A. Meguid, Advances in the development of superhydrophobic and icephobic surfaces, Int. J. Mech. Mater. Des. 18 (3) (2022) 509–547.

[16] S.S. Latthe, R.S. Sutar, A.K. Bhosale, S. Nagappan, C.-S. Ha, K.K. Sadasivuni, S. Liu, R. Xing, Recent developments in air-trapped superhydrophobic and liquid-infused slippery surfaces for anti-icing application, Prog. Org. Coat. 137 (2019), 105373.

[17] Q. Zeng, H. Zhou, J. Huang, Z. Guo, Review on the recent development of durable superhydrophobic materials for practical applications, Nanoacale 13 (2021), 11734.

[18] M. Shahid, S. Maiti, R.V. Adivarekar, S. Liu, Biomaterial based fabrication of superhydrophobic textiles-A review, Mater. Today Chem. 24 (2022), 100940.

[19] T. Young, An essay on the cohesion of fluids, Philos. Trans. 95 (1805) 65–87.

[20] R.N. Wenzel, Resistance of solid surfaces to wetting by water, Ind. Eng. Chem. 28 (1936) 988–994.

[21] A.B.D. Cassie, S. Baxter, Wettability of porous surfaces, Trans. Faraday Soc. 40 (1944) 546–551.

[22] H. Zhou, H. Niu, H. Wang, T. Lin, Self-healing superwetting surfaces, their fabrications, and properties, Chem. Rev. 123 (2023) 663–700.

[23] G. Jiang, L. Chen, S. Zhang, H. Huang, Superhydrophobic SiC/CNTs coatings with photothermal deicing and passive anti-icing properties, ACS Appl. Mater. Interfaces 10 (42) (2018) 36505–36511.

[24] S. Tan, X. Han, S. Cheng, P. Guo, X. Wang, P. Che, R. Jin, L. Jiang, L. Heng, Photothermal solid slippery surfaces with rapid self-healing, improved anti/de-Icing and excellent stability, Macromol. Rapid Commun. 44 (2023), e2200816.

[25] F. Zhang, D. Xu, D. Zhang, L. Ma, J. Wang, Y. Huang, M. Chen, H. Qian, X. Li, A durable and photothermal superhydrophobic coating with entwinned CNTs-SiO$_2$ hybrids for anti-icing applications, Chem. Eng. J. 423 (2021), 130238.

[26] W. Zheng, J. Huang, S. Li, M. Ge, L. Teng, Z. Chen, Y. Lai, Advanced materials with special wettability toward intelligent oily wastewater remediation, ACS Appl. Mater. Interfaces 13 (2021) 67–87.

[27] H. Niu, J. Li, X. Wang, F. Luo, Z. Qiang, J. Ren, Solar-assisted, fast, and in situ recovery of crude oil spill by a superhydrophobic and photothermal sponge, ACS Appl. Mater. Interfaces 13 (18) (2021) 21175–21185.

[28] P. Wang, J. Zhang, H. Wen, Z. Zhu, W. Huang, C. Liu, Photothermal conversion-assisted oil water separation by superhydrophobic cotton yarn prepared via the

silver mirror reaction, Colloids Surf. A Physicochem. Eng. Aspects 610 (2021), 125684.

[29] C. Zhang, M.-B. Wu, B.-H. Wu, J. Yang, Z.-K. Xu, Solar-driven self-heating sponges for highly efficient crude oil spill remediation, J. Mater. Chem. A 6 (19) (2018) 8880–8885.

[30] J. Liu, H. Guo, Z. Sun, B. Li, Preparation of photothermal membrane for vacuum membrane distillation with excellent anti-fouling ability through surface spraying, J. Membr. Sci. 634 (2021), 119434.

[31] W.-T. Cao, W. Feng, Y.-Y. Jiang, C. Ma, Z.-F. Zhou, M.-G. Ma, Y. Chen, F. Chen, Two-dimensional MXene-reinforced robust surface superhydrophobicity with self-cleaning and photothermal-actuating binary effects, Mater. Horiz. 6 (5) (2019) 1057–1065.

[32] C.-H. Xue, Y. Wu, X.-J. Guo, B.-Y. Liu, H.-D. Wang, S.-T. Jia, Superhydrophobic, flame-retardant and conductive cotton fabrics via layer-by-layer assembly of carbon nanotubes for flexible sensing electronics, Cellulose 27 (6) (2020) 3455–3468.

[33] F. Wang, L. Wang, H. Wu, J. Pang, D. Gu, S. Li, A lotus-leaf-like SiO₂ superhydrophobic bamboo surface based on soft lithography, Colloids Surf. A Physicochem. Eng. Aspects 520 (2017) 834–840.

[34] L.B. Boinovich, E.B. Modin, A.R. Sayfutdinova, K.A. Emelyanenko, A.L. Vasiliev, A.M. Emelyanenko, Combination of functional nanoengineering and nanosecond laser texturing for design of superhydrophobic aluminum alloy with exceptional mechanical and chemical properties, ACS Nano 11 (2017) 10113–10123.

[35] T.T. Isimjan, T. Wang, S. Rohani, A novel method to prepare superhydrophobic, UV resistance and anti-corrosion steel surface, Chem. Eng. J. 210 (2012) 182–187.

[36] E. Sharifikolouei, Z. Najmi, A. Cochis, A.C. Scalia, M. Aliabadi, S. Perero, L. Rimondini, Generation of cytocompatible superhydrophobic Zr-Cu-Ag metallic glass coatings with antifouling properties for medical textiles, Mater, Today Bio 12 (2021), 100148.

[37] M.M. Aljumaily, M.A. Alsaadi, R. Das, S.B.A. Hamid, N.A. Hashim, M.K. AlOmar, H.M. Alayan, M. Novikov, Q.F. Alsalhy, M.A. Hashim, Optimization of the synthesis of superhydrophobic carbon nanomaterials by chemical vapor deposition, Sci. Rep. 8 (2018) 2778.

[38] L. Liu, G. Kong, Y. Zhu, C. Che, Superhydrophobic graphene aerogel beads for adsorption of oil and organic solvents via a convenient in situ sol-gel method, Colloid Interface Sci. Commun. 45 (2021), 100518.

[39] X. Cui, Q. Ruan, X. Zhuo, X. Xia, J. Hu, R. Fu, Y. Li, J. Wang, H. Xu, Photothermal nanomaterials: a powerful light-to-heat converter, Chem. Rev. 123 (2023) 6891–6952.

[40] Y. Wu, H. Huang, W. Zhou, C. You, H. Ye, J. Chen, S. Zang, J. Yun, X. Chen, L. Wang, Z. Yuan, High-porosity lamellar films prepared by a multistage assembly strategy for efficient photothermal water evaporation and power generation, ACS Appl. Mater. Interfaces 14 (25) (2022) 29099–29110.

[41] C. Chen, Y. Kuang, L. Hu, Challenges and opportunities for solar evaporation, Joule 3 (3) (2019) 683–718.

[42] P. Zijlstra, P.M. Paulo, M. Orrit, Optical detection of single non-absorbing molecules using the surface plasmon resonance of a gold nanorod, Nat. Nanotechnol. 7 (6) (2012) 379–382.

[43] D. Xu, Z. Li, L. Li, J. Wang, Insights into the photothermal conversion of 2D MXene nanomaterials: synthesis, mechanism, and applications, Adv. Funct. Mater. 30 (47) (2020), 2000712.

[44] N.S. Fuzil, N.H. Othman, N.H. Alias, F. Marpani, M.H.D. Othman, A.F. Ismail, W. J. Lau, K. Li, T.D. Kusworo, I. Ichinose, A review on photothermal material and its usage in the development of photothermal membrane for sustainable clean water production, Desalination 517 (2021), 115259.

[45] P. Cheng, D. Wang, P. Schaaf, A review on photothermal conversion of solar energy with nanomaterials and nanostructures: from fundamentals to applications, Adv. Sust. Syst. 6 (9) (2022), 2200115.

[46] J. Qiu, M. Xie, T. Wu, D. Qin, Y. Xia, Gold nanocages for effective photothermal conversion and related applications, Chem. Sci. 11 (48) (2020) 12955–12973.

[47] M. Chen, Y. He, J. Huang, J. Zhu, Investigation into Au nanofluids for solar photothermal conversion, Int. J. Heat Mass Transf. 108 (2017) 1894–1900.

[48] X.M. Zhu, H.Y. Wan, H. Jia, L. Liu, J. Wang, Porous Pt nanoparticles with high near-infrared photothermal conversion efficiencies for photothermal therapy, Adv. Healthcare Mater. 5 (24) (2016) 3165–3172.

[49] Z.W. Seh, S. Liu, M. Low, S.Y. Zhang, Z. Liu, A. Mlayah, M.Y. Han, Janus Au-TiO₂ photocatalysts with strong localization of plasmonic near-fields for efficient visible-light hydrogen generation, Adv. Mater. 24 (17) (2012) 2310–2314.

[50] Y. Liu, J. Zhao, S. Zhang, D. Li, X. Zhang, Q. Zhao, B. Xing, Advances and challenges of broadband solar absorbers for efficient solar steam generation, Environ. Sci.: Nano 9 (7) (2022) 2264–2296.

[51] L. Wang, D. Wang, Z. Wu, J. Luo, X. Huang, Q. Gao, X. Lai, L.C. Tang, H. Xue, J. Gao, Self-derived superhydrophobic and multifunctional polymer sponge composite with excellent joule heating and photothermal performance for strain/pressure sensors, ACS Appl. Mater. Interfaces 12 (11) (2020) 13316–13326.

[52] M. Wu, Y. Li, N. An, J. Sun, Applied voltage and near-infrared light enable healing of superhydrophobicity loss caused by severe scratches in conductive superhydrophobic films, Adv. Funct. Mater. 26 (37) (2016) 6777–6784.

[53] F. Tao, J. Zheng, L. Wang, Y. Yuan, F. Wan, W. Xu, Z. Huang, S. Wang, Y. Huang, Plasmonic photothermal film for defogging and anti-icing/deicing on PTFE, J. Alloys Compd. 866 (2021), 158827.

[54] N. Li, Y. Zhang, H. Zhi, J. Tang, Y. Shao, L. Yang, T. Sun, H. Liu, G. Xue, Micro/nano-cactus structured aluminium with superhydrophobicity and plasmon-enhanced photothermal trap for icephobicity, Chem. Eng. J. 429 (2022), 132183.

[55] W. Zhao, L. Xiao, X. He, Z. Cui, J. Fang, C. Zhang, X. Li, G. Li, L. Zhong, Y. Zhang, Moth-eye-inspired texturing surfaces enabled self-cleaning aluminum to achieve photothermal anti-icing, Opt. Laser Technol. 141 (2021), 107115.

[56] S. Kumar, M. Karmacharya, S.R. Joshi, O. Gulenko, J. Park, G.H. Kim, Y.K. Cho, Photoactive antiviral face mask with self-sterilization and reusability, Nano Lett. 21 (2021) 337–343.

[57] L. Ding, Y. Chang, P. Yang, W. Gao, M. Sun, Y. Bie, L. Yang, X. Ma, Y. Guo, Facile synthesis of biocompatible L-cysteine-modified MoS₂ nanospheres with high photothermal conversion efficiency for photothermal therapy of tumor, Mater. Sci. Eng. 117 (2020), 111371.

[58] J. Wang, Y. Li, L. Deng, N. Wei, Y. Weng, S. Dong, D. Qi, J. Qiu, X. Chen, T. Wu, High-performance photothermal conversion of narrow-bandgap Ti₂O₃ nanoparticles, Adv. Mater. 29 (3) (2017), 201603730.

[59] A. Sennaroglu, M. Khan, M. Hashemkhani, H. Yagci Acar, Determination of the wavelength-dependent photothermal conversion efficiency of photosensitizers for photothermal therapy: application to Ag₂S-glutathione quantum dots, J. Phys. Chem. B 125 (42) (2021) 11650–11659.

[60] C.M. Hessel, V.P. Pattani, M. Rasch, M.G. Panthani, B. Koo, J.W. Tunnell, B. A. Korgel, Copper selenide nanocrystals for photothermal therapy, Nano Lett. 11 (6) (2011) 2560–2566.

[61] X. Yin, Y. Zhang, D. Wang, Z. Liu, Y. Liu, X. Pei, B. Yu, F. Zhou, Integration of self-lubrication and near-infrared photothermogenesis for excellent anti-icing/deicing performance, Adv. Funct. Mater. 25 (27) (2015) 4237–4245.

[62] T. Cheng, R. He, Q. Zhang, X. Zhan, F. Chen, Magnetic particle-based super-hydrophobic coatings with excellent anti-icing and thermoresponsive deicing performance, J. Mater. Chem. A 3 (43) (2015) 21637–21646.

[63] R.L. Yang, Y.J. Zhu, D.D. Qin, Z.C. Xiong, Light-operated dual-mode propulsion at the liquid/air interface using flexible, superhydrophobic, and thermally stable photothermal paper, ACS Appl. Mater. Interfaces 12 (1) (2020) 1339–1347.

[64] L. Ma, J. Wang, F. Zhao, D. Wu, Y. Huang, D. Zhang, Z. Zhang, W. Fu, X. Li, Y. Fan, Plasmon-mediated photothermal and superhydrophobic TiN-PTFE film for anti-icing/deicing applications, Compos. Sci. Technol. 181 (2019), 107696.

[65] H. Xie, W.H. Xu, C. Fang, T. Wu, Efficient and economical approach for flexible photothermal icephobic copper mesh with robust superhydrophobicity and active deicing property, Soft Matter 17 (7) (2021) 1901–1911.

[66] H. Ni, Z. Gao, X. Li, Y. Xiao, Y. Wang, Y. Zhang, Synthesis and characterization of CuFeMnO₄ prepared by co-precipitation method, J. Mater. Sci. 53 (5) (2017) 3581–3589.

[67] M. Wang, T. Yang, G. Cao, X. Wang, Z. Jiang, C. Wang, Y. Li, Simulation-guided construction of solar thermal coating with enhanced light absorption capacity for effective icephobicity, Chem. Eng. J. 408 (2021), 127316.

[68] A. Sun, X. Hou, X. Hu, Super-performance photothermal conversion of 3D macrostructure graphene-CuFeSe₂ aerogel contributes to durable and fast clean-up of highly viscous crude oil in seawater, Nano Energy 70 (2020), 104511.

[69] M. Ghidiu, M.R. Lukatskaya, M.Q. Zhao, Y. Gogotsi, M.W. Barsoum, Conductive two-dimensional titanium carbide 'clay' with high volumetric capacitance, Nature 516 (7529) (2014) 78–81.

[70] L. Ding, Y. Wei, Y. Wang, H. Chen, J. Caro, H. Wang, A two-dimensional lamellar membrane: MXene nanosheet stacks, Angew. Chem. 56 (7) (2017) 1825–1829.

[71] R. Li, L. Zhang, L. Shi, P. Wang, MXene Ti₃C₂: an effective 2D light-to-heat conversion material, ACS Nano 11 (4) (2017) 3752–3759.

[72] M. Wang, J. Zhu, Y. Zi, W. Huang, 3D MXene sponge: facile synthesis, excellent hydrophobicity, and high photothermal efficiency for waste oil collection and purification, ACS Appl. Mater. Interfaces 13 (39) (2021) 47302–47312.

[73] J. Luo, S. Gao, H. Luo, L. Wang, X. Huang, Z. Guo, X. Lai, L. Lin, R.K.Y. Li, J. Gao, Superhydrophobic and breathable smart MXene-based textile for multifunctional wearable sensing electronics, Chem. Eng. J. 406 (2021), 126898.

[74] Q. Zhang, G. Yi, Z. Fu, H. Yu, S. Chen, X. Quan, Vertically aligned Janus MXene-based aerogels for solar desalination with high efficiency and salt resistance, ACS Nano 13 (11) (2019) 13196–13207.

[75] Y. Li, Y. Shi, H. Wang, T. Liu, X. Zheng, S. Gao, J. Lu, Recent Advances in Carbon-based Materials for Solar-driven Interfacial Photothermal Conversion Water Evaporation: Assemblies, Structures, Applications, and Prospective, Carbon Energy, 2023, p. e331.

[76] Q. Zhang, W. Xu, X. Wang, Carbon nanocomposites with high photothermal conversion efficiency, Sci. China Mater. 61 (7) (2018) 905–914.

[77] Y. Hu, Y. Jiang, L. Ni, Z. Huang, L. Liu, Q. Ke, H. Xu, An elastic MOF/graphene aerogel with high photothermal efficiency for rapid removal of crude oil, J. Hazard. Mater. 443 (Pt B) (2023), 130339.

[78] J. Zhang, X. Zhao, J. Wei, B. Li, J. Zhang, Superhydrophobic coatings with photothermal self-healing chemical composition and microstructure for efficient corrosion protection of magnesium alloy, Langmuir 37 (45) (2021) 13527–13536.

[79] C.-H. Xue, M.-M. Du, X.-J. Guo, B.-Y. Liu, R.-X. Wei, H.-G. Li, M.-C. Huang, F.-Q. Deng, S.-T. Jia, Fabrication of superhydrophobic photothermal conversion fabric via layer-by-layer assembly of carbon nanotubes, Cellulose 28 (8) (2021) 5107–5121.

[80] Y. Liu, Y. Wu, Y. Liu, R. Xu, S. Liu, F. Zhou, Robust photothermal coating strategy for efficient ice removal, ACS Appl. Mater. Interfaces 12 (41) (2020) 46981–46990.

[81] Y. Fu, F. Xu, D. Weng, X. Li, Y. Li, J. Sun, Superhydrophobic foams with chemical - and mechanical-damage-healing abilities enabled by self-healing polymers, ACS Appl. Mater. Interfaces 11 (40) (2019) 37285–37294.

[82] X. Su, H. Li, X. Lai, Z. Yang, Z. Chen, W. Wu, X. Zeng, Vacuum-assisted layer-by-layer superhydrophobic carbon nanotube films with electrothermal and photothermal effects for deicing and controllable manipulation, J. Mater. Chem. A 6 (35) (2018) 16910–16919.

[83] N. Jiang, Y. Wang, K.C. Chan, C.Y. Chan, H. Sun, G. Li, Additive manufactured graphene coating with synergistic photothermal and superhydrophobic effects for bactericidal applications, Glob. Chall. 4 (1) (2020) 1900054.

[84] X. Wang, L. Dai, N. Jiao, S. Tung, L. Liu, Superhydrophobic photothermal graphene composites and their functional applications in microrobots swimming at the air/water interface, Chem. Eng. J. 422 (2021), 129394.

[85] H. Zhong, Z. Zhu, J. Lin, C.F. Cheung, V.L. Lu, F. Yan, C.Y. Chan, G. Li, Reusable and recyclable graphene masks with outstanding superhydrophobic and photothermal performances, ACS Nano 14 (5) (2020) 6213–6221.

[86] Q. Zhao, W. Yang, Y. Li, Z. He, Y. Li, Y. Zhou, R. Wang, J. Fan, K. Zhang, Multifunctional phase change microcapsules based on graphene oxide Pickering emulsion for photothermal energy conversion and superhydrophobicity, Int. J. Energy Res. 44 (6) (2020) 4464–4474.

[87] Y.T. Li, H. Chen, R. Deng, M.B. Wu, H.C. Yang, S.B. Darling, Sandwich-structured photothermal wood for durable moisture harvesting and pumping, ACS Appl. Mater. Interfaces 13 (28) (2021) 33713–33721.

[88] W. Zheng, L. Teng, Y. Lai, T. Zhu, S. Li, X. Wu, W. Cai, Z. Chen, J. Huang, Magnetic responsive and flexible composite superhydrophobic photothermal film for passive anti-icing/active deicing, Chem. Eng. J. 427 (2022), 130922.

[89] S. Wu, Y. Du, Y. Alsaid, D. Wu, M. Hua, Y. Yan, B. Yao, Y. Ma, X. Zhu, X. He, Superhydrophobic photothermal icephobic surfaces based on candle soot, Proc. Natl. Acad. Sci. U.S.A. 117 (21) (2020) 11240–11246.

[90] Z. Xie, H. Wang, Y. Geng, M. Li, Q. Deng, Y. Tian, R. Chen, X. Zhu, Q. Liao, Carbon-based photothermal superhydrophobic materials with hierarchical structure enhances the anti-icing and photothermal deicing properties, ACS Appl. Mater. Interfaces 13 (40) (2021) 48308–48321.

[91] Y. Kong, S. Zhang, Y. Gao, X. Cheng, W. Kong, Y. Qi, S. Wang, F. Yin, Z. Dai, Q. Yue, B. Gao, Low-temperature carbonization synthesis of carbon-based super-hydrophobic foam for efficient multi-state oil/water separation, J. Hazard Mater. 423 (Pt B) (2022), 127064.

[92] X. Jia, X. Liu, H. Guan, T. Fan, Y. Chen, Y.-Z. Long, A loofah-based photothermal biomass material with high salt-resistance for efficient solar water evaporation, Compos. Commun. 37 (2023), 101430.

[93] Z. Liu, F. Feng, Y. Li, Y. Sun, K. Tagawa, A corncob biochar-based superhydrophobic photothermal coating with micro-nano-porous rough-structure for ice-phobic properties, Surf. Coat. Technol. 457 (2023), 129299.

[94] H. Xie, J. Wei, S. Duan, Q. Zhu, Y. Yang, K. Chen, J. Zhang, L. Li, J. Zhang, Non-fluorinated and durable photothermal superhydrophobic coatings based on attapulgite nanorods for efficient anti-icing and deicing, Chem. Eng. J. 428 (2022), 132585.

[95] R. Li, G. Zhang, L. Yang, C. Zhou, Superhydrophobic polyaniline absorbent for solar-assisted adsorption of highly viscous crude oil, Sep. Purif. Technol. 276 (2021), 119372.

[96] M. Wu, S. Ding, L. Deng, X. Wang, PPy nanotubes-enabled in-situ heating nanofibrous composite membrane for solar-driven membrane distillation, Sep. Purif. Technol. 281 (2022), 119995.

[97] Y. Yang, Z. Guo, W. Lin, Robust mussel-inspired superhydrophobic sponge with eco-friendly photothermal effect for crude oil/seawater separation, J. Hazard Mater. 461 (2024), 132592.

[98] J. He, Y. Wu, G. Cao, L. Shen, Y. Lv, B. Zhang, J. Ge, M. Qu, Solar-assisted, highly efficient, and in situ recovery of crude oil spill by a FeCo$_2$S$_4$ modified sponge, Adv. Eng. Mater. (2022) 220435.

[99] C. Shen, Y. Zhu, X. Xiao, X. Xu, X. Chen, G. Xu, Economical salt-resistant superhydrophobic photothermal membrane for highly efficient and stable solar desalination, ACS Appl. Mater. Interfaces 12 (31) (2020) 35142–35151.

[100] X. Guo, H. Gao, S. Wang, L. Yin, Y. Dai, Scalable, flexible and reusable graphene oxide-functionalized electrospun nanofibrous membrane for solar photothermal desalination, Desalination 488 (2020), 114535.

[101] J. Huang, Y. Hu, Y. Bai, Y. He, J. Zhu, Novel solar membrane distillation enabled by a PDMS/CNT/PVDF membrane with localized heating, Desalination 489 (2020), 114529.

[102] M. Gao, C.K. Peh, F.L. Meng, G.W. Ho, Photothermal membrane distillation toward solar water production, Small Methods 5 (2021) 2001200.

[103] Q. Li, X. Zhao, L. Li, T. Hu, Y. Zhang, J. Zhang, Facile preparation of polydimethylsiloxane/carbon nanotubes modified melamine solar evaporators for efficient steam generation and desalination, J. Colloid Interface Sci. 584 (2021) 602–609.

[104] T. Hu, L. Li, Y. Yang, J. Zhang, A yolk@shell superhydrophobic/superhydrophilic solar evaporator for efficient and stable desalination, J. Mater. Chem. A 8 (29) (2020) 14736–14745.

[105] C. Chen, M. Wang, X. Chen, X. Chen, Q. Fu, H. Deng, Recent progress in solar photothermal steam technology for water purification and energy utilization, Chem. Eng. J. 448 (2022), 137603.

[106] M. Gao, P.K.N. Conner, G.W. Ho, Plasmonic photothermic directed broadband sunlight harnessing for seawater catalysis and desalination, Energy Environ. Sci. 9 (2016) 3151–3160.

[107] M. Gao, L. Zhu, C.K. Peh, G.W. Ho, Solar absorber material and system designs for photothermal water vaporization towards clean water and energy production, Energy Environ. Sci. 12 (2019) 841.

[108] Y. Tian, C. Du, S. Yong, X. Zhou, C. Zhou, S. Yang, Catalysis-involved 3D N-doped graphene aerogel achieves a superior solar water purification rate and efficiency, Chem. Eng. J. 453 (2023), 139793.

[109] Y. Wang, L. Zhang, P. Wang, Self-floating carbon nanotube membrane on macroporous silica substrate for highly efficient solar-driven interfacial water evaporation, ACS Sustainable Chem. Eng. 4 (3) (2016) 1223–1230.

[110] D. Weng, F. Xu, X. Li, Y. Li, J. Sun, Bioinspired photothermal conversion coatings with self-healing superhydrophobicity for efficient solar steam generation, J. Mater. Chem. A 6 (47) (2018) 24441–24451.

[111] E. Li, Y. Pan, C. Wang, C. Liu, C. Shen, C. Pan, X. Liu, Asymmetric superhydrophobic textiles for electromagnetic interference shielding, photothermal conversion, and solar water evaporation, ACS Appl. Mater. Interfaces 13 (24) (2021) 28996–29007.

[112] C. Zhang, P. Xiao, F. Ni, J. Gu, J. Chen, Y. Nie, S.-W. Kuo, T. Chen, Breathable and superhydrophobic photothermic fabric enables efficient interface energy management via confined heating strategy for sustainable seawater evaporation, Chem. Eng. J. 428 (2022), 131142.

[113] S. Sun, Z.-H. Chen, Q.-R. Xiao, Multifunctional cotton fabric with favorable hydrophobicity, electrical conductivity and photothermal effect for contaminants removal and oil detection, Appl. Surf. Sci. 612 (2023), 155731.

[114] S. Zhang, J. Chen, J. Zheng, X. Chen, H. Xu, F.I.T. Petrescu, L.M. Ungureanu, Y. Li, G. Shi, A simple polypyrrole/polyvinylidene fluoride membrane with hydrophobic and self-floating ability for solar water evaporation, Nanomaterials 12 (5) (2022) 859.

[115] L. Zhang, X. Wang, X. Xu, J. Yang, J. Xiao, B. Bai, Q. Wang, A Janus solar evaporator with photocatalysis and salt resistance for water purification, Sep. Purif. Technol. 298 (2022) 121643.

[116] Y. Shang, B. Li, C. Xu, R. Zhang, Y. Wang, Biomimetic Janus photothermal membrane for efficient interfacial solar evaporation and simultaneous water decontamination, Sep. Purif. Technol. 298 (2022) 121597.

[117] X. Qiu, H. Kong, Y. Li, Q. Wang, Y. Wang, Interface engineering of a Ti$_4$O$_7$ nanofibrous membrane for efficient solar-driven evaporation, ACS Appl. Mater. Interfaces 14 (2022) 54855–54866.

[118] C. Ma, L. He, R. Liu, H. Guan, C. Ge, X. Zhang, Preparation of polypyrrole/boron nitride composites and composite sponges for efficient photothermal utilization, ChemistrySelect 7 (26) (2022), e202201244.

[119] J. Jiang, H. Jiang, Y. Xu, M. Chen, L. Ai, Janus Co@C/NCNT photothermal membrane with multiple optical absorption for highly efficient solar water evaporation and wastewater purification, Colloids Surf. A Physicochem. Eng. Aspects 647 (2022), 128960.

[120] H. Xie, Y. Du, W. Zhou, Y. Wang, C. Zhang, R. Niu, T. Wu, J. Qu, Efficient Fabrication of Micro/nanostructured Polyethylene/carbon Nanotubes Foam with Robust Superhydrophobicity, Excellent Photothermality, and Sufficient Adaptability for All-Weather Freshwater Harvesting, Small, 2023, e2300915.

[121] X. Cheng, Y. Kong, Y. Gao, H. Dan, Y. Wei, W. Yin, B. Gao, Q. Yue, One-step construction of P(AM-DMDAAC)/GO aerogel evaporator with Janus wettability for stable solar-driven desalination, Sep. Purif. Technol. 303 (2022) 122285.

[122] Y. Lin, H. Chen, G. Wang, A. Liu, Recent progress in preparation and anti-icing applications of superhydrophobic coatings, Coatings 8 (6) (2018) 208.

[123] J. Hu, G. Jiang, Superhydrophobic coatings on iodine doped substrate with photothermal deicing and passive anti-icing properties, Surf. Coat. Technol. 402 (2020), 126342.

[124] B. Wu, X. Cui, H. Jiang, N. Wu, C. Peng, Z. Hu, X. Liang, Y. Yan, J. Huang, D. Li, A superhydrophobic coating harvesting mechanical robustness, passive anti-icing and active de-icing performances, J. Colloid Interface Sci. 590 (2021) 301–310.

[125] Q. Li, Z. Guo, Fundamentals of icing and common strategies for designing biomimetic anti-icing surfaces, J. Mater. Chem. A 6 (28) (2018) 13549–13581.

[126] C.-H. Xue, H.-G. Li, X.-J. Guo, Y.-R. Ding, B.-Y. Liu, Q.-F. An, Y. Zhou, Superhydrophobic anti-icing coatings with self-deicing property using melanin nanoparticles from cuttlefish juice, Chem. Eng. J. 424 (2021) 130553.

[127] B. Yu, Z. Sun, Y. Liu, Z. Zhang, Y. Wu, F. Zhou, Improving anti-icing and de-icing performances via thermal-regulation with macroporous xerogel, ACS Appl. Mater. Interfaces 13 (31) (2021) 37609–37616.

[128] D. Wu, L. Ma, F. Zhang, H. Qian, B. Minhas, Y. Yang, X. Han, D. Zhang, Durable deicing lubricant-infused surface with photothermally switchable hydrophobic/slippery property, Mater. Des. 185 (2020), 108236.

[129] R. Zhu, M. Liu, Y. Hou, L. Zhang, M. Li, D. Wang, S. Fu, One-pot preparation of fluorine-free magnetic superhydrophobic particles for controllable liquid marbles and robust multifunctional coatings, ACS Appl. Mater. Interfaces 12 (14) (2020) 17004–17017.

[130] S. Zhang, F. Zhang, Z. Zhang, G. Li, H. Fu, J. Huang, Y. Wang, Z. Lei, X. Qian, Y. Lai, An electroless nickel plating fabric coated with photothermal Chinese ink for powerful passive anti-icing/icephobic and fast active deicing, Chem. Eng. J. 450 (2022), 138328.

[131] Z. Xie, H. Wang, Q. Deng, Y. Tian, Y. Shao, R. Chen, X. Zhu, Q. Liao, Heat transfer characteristics of carbon-based photothermal superhydrophobic materials with thermal insulation micropores during anti-icing/deicing, J. Phys. Chem. Lett. 13 (43) (2022) 10237–10244.

[132] B. Wang, P. Yu, Q. Wang, Z. Jing, W. Wang, P. Li, X. Tong, F. Lin, D. Wang, G. E. Lio, R. Caputo, O. Ávalos-Ovando, A.O. Govorov, H. Xu, Z.M. Wang, Upcycling of biomass waste into photothermal superhydrophobic coating for efficient anti-icing and deicing, Mater. Today Phys. 24 (2022), 100683.

[133] Y. Tian, Y. Xu, Z. Zhu, Y. Liu, J. Xie, B. Zhang, H. Zhang, Q. Zhang, Hierarchical micro/nano/porous structure PVDF/hydrophobic GO photothermal membrane with highly efficient anti-icing/de-icing performance, Colloids Surf. A Physicochem. Eng. Aspects 651 (2022), 129586.

[134] Y. Liu, Y. Shao, Y. Wang, J. Wang, An abrasion-resistant, photothermal, superhydrophobic anti-icing coating prepared by polysiloxane-modified carbon nanotubes and fluorine-silicone resin, Colloids Surf. A Physicochem. Eng. Aspects 648 (2022), 129335.

[135] Z. Zhu, S. Fu, L.A. Lucia, A fiber-aligned thermal-managed wood-based superhydrophobic aerogel for efficient oil recovery, ACS Sustainable Chem. Eng. 7 (19) (2019) 16428–16439.

[136] Y. Wang, L. Zhou, X. Luo, Y. Zhang, J. Sun, X. Ning, Y. Yuan, Solar-heated graphene sponge for high-efficiency clean-up of viscous crude oil spill, J. Clean. Prod. 230 (2019) 995–1002.

[137] S. Liu, Q. Xu, S.S. Latthe, A.B. Gurav, R. Xing, Superhydrophobic/superoleophilic magnetic polyurethane sponge for oil/water separation, RSC Adv. 5 (84) (2015) 68293–68298.

[138] C. Yang, B. Bai, Y. He, N. Hu, H. Wang, Y. Suo, Novel fabrication of solar light-heated sponge through polypyrrole modification method and their applications for fast cleanup of viscous oil spills, Ind. Eng. Chem. Res. 57 (14) (2018) 4955–4966.

[139] H. Saini, E. Otyepková, A. Schneemann, R. Zbořil, M. Otyepka, R.A. Fischer, K. Jayaramulu, Hierarchical porous metal–organic framework materials for efficient oil–water separation, J. Mater. Chem. A 10 (6) (2022) 2751–2785.

[140] A. Raj, R.M. Rego, K.V. Ajeya, H.-Y. Jung, T. Altalhi, G.M. Neelgund, M. Kigga, M. D. Kurkuri, Underwater oleophobic-super hydrophilic strontium-MOF for efficient oil/water separation, Chem. Eng. J. 453 (2023), 139757.

[141] M. Wang, Z. Zhang, Y. Wang, X. Zhao, X. Men, M. Yang, Ultrafast fabrication of metal-organic framework-functionalized superwetting membrane for multichannel oil/water separation and floating oil collection, ACS Appl. Mater. Interfaces 12 (22) (2020) 25512–25520.

[142] Y. Zhu, H. Li, W. Huang, X. Lai, X. Zeng, Facile fabrication of superhydrophobic wood aerogel by vapor deposition method for oil-water separation, Surf. Interfaces 37 (2023), 102746.

[143] G. Wang, Y. Xu, R. Zhang, S. Gai, Y. Zhao, F. Yang, K. Cheng, Fire-resistant MXene composite aerogels for effective oil/water separation, J. Environ. Chem. Eng. 11 (1) (2023), 109127.

[144] Z. Tan, L. Hu, D. Yang, D. Zheng, X. Qiu, Lignin: excellent hydrogel swelling promoter used in cellulose aerogel for efficient oil/water separation, J. Colloid Interface Sci. 629 (Pt A) (2023) 422–433.

[145] W. Chao, S. Wang, Y. Li, G. Cao, Y. Zhao, X. Sun, C. Wang, S.-H. Ho, Natural sponge-like wood-derived aerogel for solar-assisted adsorption and recovery of high-viscous crude oil, Chem. Eng. J. 400 (2020), 125865.

[146] K. Wang, D.Y. Wang, M.Z. Wang, X.X. Dan, L.M. Che, H.H. Xu, H. Zhou, H. Liu, L. Singh, X.E. Wu, Functional photothermal sponges for efficient solar steam generation and accelerated cleaning of viscous crude-oil spill, Sol. Energy Mater. Sol. Cells 204 (2020), 110203.

[147] C. Zhang, Y. Li, S. Sun, M. Kalulu, Y. Wang, X. Zhou, X. Wang, Q. Du, Y. Jiang, Novel magnetic and flame-retardant superhydrophobic sponge for solar-assisted high-viscosity oil/water separation, Prog. Org. Coat. 139 (2020), 105369.

[148] J. Chang, Y. Shi, M. Wu, R. Li, L. Shi, Y. Jin, W. Qing, C. Tang, P. Wang, Solar-assisted fast cleanup of heavy oil spills using a photothermal sponge, J. Mater. Chem. A 6 (19) (2018) 9192–9199.

[149] Z. Luo, X. Wang, D. Yang, S. Zhang, T. Zhao, L. Qin, Z.Z. Yu, Photothermal hierarchical carbon nanotube/reduced graphene oxide microspherical aerogels with radially orientated microchannels for efficient cleanup of crude oil spills, J. Colloid Interface Sci. 570 (2020) 61–71.

[150] X. Wu, Y. Lei, S. Li, J. Huang, L. Teng, Z. Chen, Y. Lai, Photothermal and Joule heating-assisted thermal management sponge for efficient cleanup of highly viscous crude oil, J. Hazard Mater. 403 (2021), 124090.

[151] Z. Guo, B. Long, S. Gao, J. Luo, L. Wang, X. Huang, D. Wang, H. Xue, J. Gao, Carbon nanofiber based superhydrophobic foam composite for high performance oil/water separation, J. Hazard Mater. 402 (2021), 123838.

[152] Y. Yan, M. He, P. Zhou, X. Zeng, X. Huang, P. Pi, S. Xu, L. Wang, X. Wen, Durable superhydrophobic sponge for all-weather cleanup of viscous crude oil by electrothermal and photothermal effects, Sep. Purif. Technol. 304 (2023), 122374.

[153] J. Ma, S. Ma, J. Xue, M. Xu, J. Zhang, J. Li, Z. Zhao, S. Zhao, J. Pan, Z. Ye, Synthesis of elastic hydrophobic biomass sponge for rapid solar-driven viscous crude-oil cleanup absorption, oil-water separation and organic pollutants treating, Separation and Purification Technology 305 (2023).

[154] J. Yu, C. Cao, S. Liu, Y. Pan, Eco-friendly magneto-photothermal sponge for the fast recovery of highly viscous crude oil spill, Sep. Purif. Technol. 298 (2022), 122512.

[155] Z. Wu, K. Zheng, Z. Cheng, S. Zhou, Solar-assisted superhydrophobic MoS_2/PDMS/MS sponge for the efficient cleanup of viscous oil, Langmuir 38 (35) (2022) 10902–10914.

[156] X. Wang, Z. Liu, X. Liu, Y. Su, J. Wang, T. Fan, X. Ning, S. Ramakrishn, Y.-Z. Long, Ultralight and multifunctional PVDF/SiO_2@GO nanofibrous aerogel for efficient harsh environmental oil-water separation and crude oil absorption, Carbon 193 (2022) 77–87.

[157] Z. Liu, M. Chen, C. Lin, F. Li, J.T. Aladejana, J. Hong, G. Zhao, Z. Qin, X. Zhu, W. Zhang, D. Chen, X. Peng, T. Chen, Solar-assisted high-efficient cleanup of viscous crude oil spill using an ink-modified plant fiber sponge, J. Hazard Mater. 432 (2022), 128740.

[158] Z. Li, Z. Lin, Q. Tian, X. Yue, F. Qiu, T. Zhang, Solar-heating superhydrophobic modified melamine sponge for efficient recovery of viscous crude oil, J. Hazard Mater. 440 (2022), 129799.

[159] H. Zhong, Z. Zhu, P. You, J. Lin, C.F. Cheung, V.L. Lu, F. Yan, C.Y. Chan, G. Li, P Plasmonic and superhydrophobic self-decontaminating N95 respirators, ACS Nano 14 (7) (2020) 8846–8854.

[160] R. Soni, S.R. Joshi, M. Karmacharya, H. Min, S.-K. Kim, S. Kumar, G.-H. Kim, Y.-K. Cho, C.Y. Lee, Superhydrophobic and self-sterilizing surgical masks spray-coated with carbon nanotubes, ACS Appl. Nano Mater. 4 (8) (2021) 8491–8499.

[161] L. Huang, S. Xu, Z. Wang, K. Xue, J. Su, Y. Song, S. Chen, C. Zhu, B.Z. Tang, R. Ye, Self-reporting and photothermally enhanced rapid bacterial killing on a laser-induced graphene mask, ACS Nano 14 (9) (2020) 12045–12053.

[162] Q. Ren, N. Yu, P. Zou, Q. He, D.K. Macharia, Y. Sheng, B. Zhu, Y. Lin, G. Wu, Z. Chen, Reusable $Cu_{(2-x)}$S-modified masks with infrared lamp-driven antibacterial and antiviral activity for real-time personal protection, Chem. Eng. J. 441 (2022), 136043.

[163] R.-L. Yang, Y.-J. Zhu, F.-F. Chen, D.-D. Qin, Z.-C. Xiong, Superhydrophobic photothermal paper based on ultralong hydroxyapatite nanowires for controllable light-driven self-propelled motion, ACS Sustainable Chem. Eng. 7 (15) (2019) 13226–13235.

[164] X. Song, X. Huang, J. Luo, B. Long, W. Zhang, L. Wang, J. Gao, H. Xue, Flexible, superhydrophobic and multifunctional carbon nanofiber hybrid membranes for high performance light driven actuators, Nanoscale 13 (27) (2021) 12017–12027.

[165] H. Wu, J. Luo, X. Huang, L. Wang, Z. Guo, J. Liang, S. Zhang, H. Xue, J. Gao, Superhydrophobic, mechanically durable coatings for controllable light and magnetism driven actuators, J. Colloid Interface Sci. 603 (2021) 282–290.